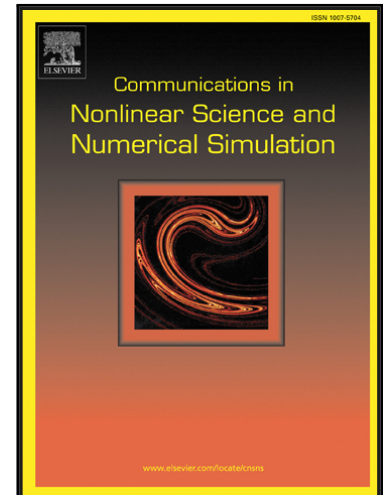


Accepted Manuscript

Heteroclinic Chaos and Its Local Suppression in Attitude Dynamics of an Asymmetrical Dual-Spin Spacecraft and Gyrostat-Satellites The Part II – The heteroclinic chaos investigation

Anton V. Doroshin

PII: S1007-5704(15)00253-1
DOI: [10.1016/j.cnsns.2015.07.006](https://doi.org/10.1016/j.cnsns.2015.07.006)
Reference: CNSNS 3612



To appear in: *Communications in Nonlinear Science and Numerical Simulation*

Received date: 18 February 2015
Revised date: 7 June 2015
Accepted date: 20 June 2015

Please cite this article as: Anton V. Doroshin , Heteroclinic Chaos and Its Local Suppression in Attitude Dynamics of an Asymmetrical Dual-Spin Spacecraft and Gyrostat-Satellites The Part II – The heteroclinic chaos investigation, *Communications in Nonlinear Science and Numerical Simulation* (2015), doi: [10.1016/j.cnsns.2015.07.006](https://doi.org/10.1016/j.cnsns.2015.07.006)

This is a PDF file of an unedited manuscript that has been accepted for publication. As a service to our customers we are providing this early version of the manuscript. The manuscript will undergo copyediting, typesetting, and review of the resulting proof before it is published in its final form. Please note that during the production process errors may be discovered which could affect the content, and all legal disclaimers that apply to the journal pertain.

Highlights

- New generalized models are obtained for the dual-spin spacecraft with the constructional/mass-inertia asymmetry.
- New action-angle-solutions for the heteroclinic case of the dynamics are found.
- The Melnikov-Wiggins formalism was used for the heteroclinic chaos analysis in the hamiltonian and non-Hamiltonian cases of the perturbations; the problems of the Melnikov-Wiggins methodology are indicated.
- Chaos suppression techniques are considered and new heteroclinic chaos suppressing schemes are suggested.

ACCEPTED MANUSCRIPT

Heteroclinic Chaos and Its Local Suppression in Attitude Dynamics of an Asymmetrical Dual-Spin Spacecraft and Gyrostat-Satellites

The Part II – The heteroclinic chaos investigation

Anton V. Doroshin

doran@inbox.ru

*Space Engineering Department,
Samara State Aerospace University (National Research University),
SSAU, 34, Moskovskoe Shosse str., Samara, 443086, Russia*

Abstract. Chaotic dynamics of the dual-spin spacecraft (DSSC) and gyrostats-satellites is analyzed at the presence of the constructional asymmetry and at the action of the internal/external perturbations, including the friction between the coaxial DSSC bodies, electromotors' torques applied to the rotor-body from the platform-body by internal engines, the counterelectromotive forces/torques in internal engines, internal plyharmonic disturbances and external magnetic perturbations. The heteroclinic chaos suppression tasks are considered basing on the Melnikov-Wiggins formalism. Some alternative chaos suppressing techniques are described.

Keywords: Dual-Spin Spacecraft, Satellite, Gyrostat, Exact Heteroclinic Solutions, Action-Angle Variables, Chaotic Dynamics, Heteroclinic Net, Melnikov-Wiggins Methodology, Poincaré Map

1. Introduction

In this (second) part of the paper we will continue to explore the attitude dynamics of the magnetized DSSC with the complex constructional/mass-inertia asymmetry focusing on chaotic aspects of the motion and basing on the models and solutions constructed in the first part of the paper. The detection of the heteroclinic chaos will be described with the use of the Melnikov-Wiggins formalism, and also the chaos suppressing techniques with the corresponding results will be presented.

The main problems, tasks and publications related to the regular/chaotic DSSC dynamics were indicated in the corresponding introduction section in the first part of the paper (The Part I – Main models and solutions). So the readers are invited to reading the first part of this paper.

Using in this paper formulas and figures have the common continued numeration for both parts of the paper; the references list is also common.

2. The mechanical and mathematical models

The mechanical and mathematical models for the DSSC attitude dynamics are presented in the first part of the research (The Part I – Main models and solutions). The readers are invited to reading the first part of the paper.

3. Chaotic dynamics analysis

Let us consider the Melnikov's-Wiggins' formalism application to the analysis of the chaotic phenomena in the DSSC attitude dynamics at the presence of perturbations. One of the important part of the analysis is to give some descriptions of the Melnikov's-Wiggins' methodology application in the connection to the possibility of the heteroclinic chaos

suppression at some conditions relatively the perturbations. It is well-known fact, the construction of the Melnikov's-Wiggins' formalism was started in the works of V.K. Melnikov (1963), where the homoclinic manifolds intersections were analytically detected, and V.I. Arnold (1964), where this analytical technique was generalized with the help of the "moustached" tori theory [Arnold (1964)]; and for multi-dimensional dynamical systems it took the useful form after works P.J. Holmes & J.E. Marsden (1983), and S. Wiggins (1988). Also here we should note the related work of V.V. Kozlov (1980), where the dynamical systems nonintegrability was investigated as the effect of the homo/heteroclinic separatix splitting at the action of perturbations.

For the further investigation we have the heteroclinic solutions for the motion parameters, including angular velocity components (2.1), the Serret-Andoyer variables (2.8), the Cartesian coordinates $\{\bar{\Delta}, \bar{\delta}\}$ and the corresponding action-angle $\{\bar{I}_\Delta, \bar{w}_\delta\}$ canonical pair (2.24). All of these solutions are needed for the correct application of S.Wiggins' (and also P.J.Holmes'-J.E.Marsden's) methodology [Wiggins (1988); Holmes & Marsden (1983)], using the natural form of the main dynamical system (1.62) with the addition of the conjunctive heteroclinic expressions (2.24) for the reciprocal transition between the Cartesian and action-angle rotating phases $\{\bar{\delta}, \bar{\Delta}\} \leftrightarrow \{\bar{w}_\delta, \bar{I}_\Delta\}$.

3.1. The Melnikov-Wiggins function structure [Wiggins (1988)]

The chaos phenomenon in the DSSC dynamical system was considered in the wide spectrum of works [e.g., Aslanov, Bao-Zeng, Chen, Doroshin, El-Gohary, Ge, Hall, Holmes, Iñarrea, Lanchares, Leung, Kuang, Meehan, Neishtadt, Or, Peng, Shirazi, Tong, et al.] – here is not any necessity to repeat the corresponding well-known results and observations. At the same time the problem of the heteroclinic chaos avoidance/suppression has been investigated in many scientific treatises, including the indicated works, but by the reason of the multiplicity of its instrumental implementation this problem can be additionally considered. Below we present one more application of the Melnikov's-Wiggins' methodology for the solution of the task of the heteroclinic chaos suppression in dynamics of the asymmetric magnetized DSSC in the neighborhood of the cylindrical precession regime under the action of perturbations.

For the purpose of the Melnikov's-Wiggins' methodology application (to choose the appropriate form of the Melnikov-Wiggins-function) we must give some preliminary comments about dynamical systems, which we constructed above and which is used in the Melnikov's-Wiggins' methodology [Wiggins (1988)-(1992)]. So, in our research we will consider two types [Wiggins (1988)] of dynamical systems: a system of the first type (System I) - the system, which has the perturbed vector field with dissipative nature, and a system of the third type (System III) – the system with Hamiltonian perturbations.

The System I [Wiggins (1988)] has the following structure:

$$\begin{cases} \dot{x} = JD_x \mathcal{H}_0(x, I) + \varepsilon g^x(x, I, w, \mu; \varepsilon); \\ \dot{I} = \varepsilon g^I(x, I, w, \mu; \varepsilon); \\ \dot{w} = \Omega(x, I) + \varepsilon g^\theta(x, I, w, \mu; \varepsilon); \end{cases} \quad (3.1)$$

where J is the symplectic matrix, μ is the parameters vector, and $(x, I, w) \in \mathbb{R}^{2n} \times \mathbb{R}^m \times T^k$; also we indicate that in the original notations [Wiggins (1988)] the phase-angle-variable w is denoted as θ .

The System III [Wiggins (1988)] is fully Hamiltonian:

$$\begin{cases} \dot{x} = JD_x \mathcal{H}_0(x, I) + \varepsilon JD_x \mathcal{H}_1(x, I, w, \mu; \varepsilon); \\ \dot{I} = -\varepsilon D_w \mathcal{H}_1(x, I, w, \mu; \varepsilon); \\ \dot{w} = D_I \mathcal{H}_0(x, I) + \varepsilon D_I \mathcal{H}_1(x, I, w, \mu; \varepsilon); \end{cases} \quad (3.2)$$

where $(x, I, w) \in \mathbb{R}^{2n} \times \mathbb{R}^m \times T^m$, and, moreover, the canonical pairs (I, w) correspond to the action-angle variables.

Now we present the Melnikov vector function for the considering systems [Wiggins (1988)]:

The system I.

$$M^{\bar{I}}(w_0, \alpha; \mu) = (M_1^{\bar{I}}(w_0, \alpha; \mu), \dots, M_n^{\bar{I}}(w_0, \alpha; \mu)), \quad (w_0, \alpha; \mu) \in T^k \times \mathbb{R}^{n-1} \times \mathbb{R}^p, \quad (3.3)$$

where

$$M_i^{\bar{I}}(w_0, \alpha; \mu) = \int_{-\infty}^{+\infty} [\langle D_x K_i, g^x \rangle + \langle D_I K_i, g^I \rangle] (q_0^{\bar{I}}(t), \mu; 0) dt - \left\langle D_I K_i(\gamma(\bar{I}), \bar{I}), \int_{-\infty}^{+\infty} g^I(q_0^{\bar{I}}(t), \mu; 0) dt \right\rangle; \quad i = 1, \dots, n \quad (3.4)$$

and $q_0^{\bar{I}}(t) = (x^{\bar{I}}(t, \alpha), \bar{I}, \int^t \Omega(x^{\bar{I}}(s, \alpha), \bar{I}) ds + w_0)$, that corresponds to the solution on the homo(hetero)clinic orbit for the selected value of the action-variable \bar{I} ; $\mathcal{H}_0 \equiv K_1, K_2, \dots, K_n$ – are the constants corresponding to the system's “first integrals”; $\langle \bullet, \bullet \rangle$ denotes the usual Euclidian inner product (scalar product); the argument $\gamma(\bar{I})$ indicates that the block $D_I K_i(\gamma(\bar{I}), \bar{I})$ is calculated at the homo(hetero)clinic fixed point corresponding to the selected value of the action-variable \bar{I} (where $\gamma(I)$ is “the curve” formed by the homo(hetero)clinic points' positions – this curve is built in the unperturbed phase space, and is parameterized by I); μ is the system parameters set; α is a parameter, which separates/distinguishes the concrete homo(hetero)clinic solution from the corresponding continuous set of such homo(hetero)clinic solutions.

The system III.

$$M^{\bar{I}}(w_0, \alpha; \mu) = (M_2^{\bar{I}}(w_0, \alpha; \mu), \dots, M_n^{\bar{I}}(w_0, \alpha; \mu), M_{n+1}^{\bar{I}}(w_0, \alpha; \mu), \dots, M_{n+m}^{\bar{I}}(w_0, \alpha; \mu)); \quad (3.5)$$

where $(w_0, \alpha; \mu) \in T^m \times \mathbb{R}^{n-1} \times \mathbb{R}^p$,

$$M_i^{\bar{I}}(w_0, \alpha; \mu) = \int_{-\infty}^{+\infty} [\langle D_x K_i, JD_x \mathcal{H}_1 \rangle - \langle D_I K_i, D_w \mathcal{H}_1 \rangle] (q_0^{\bar{I}}(t), \mu; 0) dt +$$

$$+ \left\langle D_x K_i(\gamma(\bar{I}), \bar{I}), \int D_w \mathcal{H}_1(q_0^{\bar{I}}(t), \mu; 0) dt \right\rangle, \quad i = 2, \dots, n; \quad (3.6)$$

$$M_i^{\bar{I}}(w_0, \alpha; \mu) = - \int_{-\infty}^{+\infty} D_{w_i} \mathcal{H}_1(q_0^{\bar{I}}(t), \mu; 0) dt, \quad i = n+1, \dots, n+m;$$

$$\text{and } q_0^{\bar{I}}(t) = \left(x^{\bar{I}}(t, \alpha), \bar{I}, \int^t D_x \mathcal{H}_0(x^{\bar{I}}(s, \alpha), \bar{I}) ds + w_0 \right). \quad (3.7)$$

Here it is important to remark [Wiggins (1988)] that we do not measure the distance between the stable and unstable split heteroclinic manifolds along the direction $(D_x K_1, 0) = (D_x \mathcal{H}, 0)$, since, for the System III, the level surfaces of $\mathcal{H}_\varepsilon = \mathcal{H} + \varepsilon \mathcal{H}_\varepsilon$ are preserved under the perturbation and the direction $(D_x K_1, 0)$ is complementary to these surfaces – by this reason the Melnikov vector does not contain the corresponding 1st component.

In the connection to the DSSC motion coordinates, for both systems we can indicate that $n=m=k=1$. Also the following correspondences take place:

$$\begin{cases} x \leftrightarrow (l, L); & I \leftrightarrow \Delta = I_\Delta; & w \leftrightarrow \delta(w_\delta); \\ g^x(x, I, w, \mu; \varepsilon) = \{g_l(l, L, I_\Delta, \delta(w_\delta)), g_L(l, L, I_\Delta, \delta(w_\delta))\}; \\ g^l(x, I, w, \mu; \varepsilon) = g_\Delta(l, L, I_\Delta, \delta(w_\delta)); & g^w(x, I, w, \mu; \varepsilon) = g_\delta(l, L, I_\Delta, \delta(w_\delta)); \\ \Omega(x, I) = D_I \mathcal{H}_0(x, I) = f_\delta(l, L, I_\Delta). \end{cases} \quad (3.8)$$

As can we see from the expressions (1.63) (taking into account (1.60), (1.61)), all of the perturbations $g_l, g_L, g_\delta, g_\Delta$ (3.8) are 2π -periodic in the δ -angle argument.

In the framework of the comments about the systems (the system I and the system III), we finally must give main statements, which divide cases of using the different systems types in the connection to the DSSC perturbed motion.

The Statement 1. If we consider the motion under the influence of the general form of the perturbations (1.63) at the presence of the non-Hamiltonian parts $(m_\Delta^f, m_\Delta^{DC})$, then we have to use the form of the System I (3.1) and (since $n=1$) the monocomponent Melnikov function $M_1^{\bar{I}}(w_0, \alpha; \mu)$ which is evaluated using (3.4) by the following manner (rejecting from our consideration the parametric arguments α and μ):

$$M_1^{\bar{I}}(w_0) = \int_{-\infty}^{+\infty} [D_I \mathcal{H}_0 \cdot g_l + D_L \mathcal{H}_0 \cdot g_L + D_\Delta \mathcal{H}_0 \cdot g_\Delta] \Big|_{q_0^{\bar{I}}(t)} dt - D_\Delta \mathcal{H}_0 \Big|_{\gamma(\bar{\Delta})} \cdot \int_{-\infty}^{+\infty} g_\Delta \Big|_{q_0^{\bar{I}}(t)} dt; \quad (3.9)$$

or, taking into account (1.63), we get

$$\begin{aligned} M_1^{\bar{I}}(w_0) &= \int_{-\infty}^{+\infty} [f_l \cdot g_L - f_L \cdot g_l + f_\delta \cdot g_\Delta] \Big|_{q_0^{\bar{I}}(t)} dt - f_\delta \Big|_{\gamma(\bar{\Delta})} \cdot \int_{-\infty}^{+\infty} g_\Delta \Big|_{q_0^{\bar{I}}(t)} dt; \\ q_0^{\bar{I}}(t) &= \left\{ \bar{l}(t), \bar{L}(t), \bar{\Delta}, \int^t f_\delta(s) ds + w_0 \right\}, \end{aligned} \quad (3.10)$$

where the phase-angle-integral in $q_0^{\bar{I}}(t)$ corresponds to the heteroclinic solution for the Cartesian angle, which also can be rewritten through the action-angle variables basing on (2.24):

$$\int^t f_\delta(s) \Big|_{\bar{l}(s), \bar{L}(s), \bar{\Delta}} ds = \bar{\delta}(t) = \bar{w}_\delta(t) - \bar{v}_\delta(t) \quad (3.11)$$

As the result we will have the following explicit heteroclinic solutions set for the Melnikov function (including expressions (2.1), (2.3) and (2.8)):

$$\begin{aligned} q_0^{\bar{l}}(t) &= \left\{ \bar{l}(t), \bar{L}(t), \bar{I}_\Delta, \int^t f_\delta(s) ds + w_0 = \bar{\delta}(t) + w_0 \right\} = \\ &= \left\{ \bar{l}(\bar{p}(t), \bar{q}(t), \bar{r}(t), \bar{\sigma}(t)), \bar{L}(\bar{p}(t), \bar{q}(t), \bar{r}(t), \bar{\sigma}(t)), \bar{\Delta}, \bar{\delta}(\bar{w}_\delta(t)) + w_0 = \bar{w}_\delta(t) - \bar{v}_\delta(t) + w_0 \right\} \end{aligned} \quad (3.12)$$

Here we fulfill the explicit separation of the “starting phase” w_0 in (3.12) from the main part of the expression for the angular variable – it means that the small redesignation (with respect to (2.24)) takes place; and, therefore, everywhere below we imply for the Melnikov-Wiggins function that:

$$\begin{cases} \bar{w}_\delta(t) = \sigma_* \cdot t; \\ \bar{\delta}(t) = \bar{w}_\delta(t) - \bar{v}_\delta(t) = \sigma_* \cdot t - \bar{v}_\delta(t) \end{cases} \quad (3.13)$$

Also in the framework of the Melnikov-Wiggins function’s structure it is worth to note [Wiggins (1988)] the equivalence in the use of the “starting phase” (w_0) and in the use of the “starting time” (t_0) at the evaluation of the Melnikov-Wiggins function basing on the variation of the angle-variable \bar{w}_δ as the main varied “sliding parameter”, because the corresponding linear recalculation of these parameters will take place. This circumstance [Wiggins (1988)] follows directly from the form of the angle-variable:

$$\begin{cases} \bar{w}_\delta(t) + w_0 = \sigma_* t + w_0; \\ \bar{w}_\delta(t + t_0) = \sigma_* [t + t_0] = \sigma_* t + w'_0; \end{cases}$$

and, therefore, the “sliding parameter” finally is shifted by the redesignated constant [Wiggins (1988)]. So, we will use the “starting phase” of the angle-variable (w_0) as the main varied “sliding parameter” in all our further evaluations.

The Statement 2. If the non-Hamiltonian perturbations are not considered in the research ($m_\Delta^f \equiv m_\Delta^{DC} \equiv 0$), then we have to use the form of the System III (3.2) and (since $n=m=1$) the monocomponent Melnikov function $M_2^{\bar{l}}(w_0, \alpha; \mu)$ which is evaluated using (3.7) by the following manner (taking into account (1.60), (1.61)):

$$M_2^{\bar{l}}(w_0) = - \int_{-\infty}^{+\infty} D_\delta \mathcal{H}_1 \Big|_{q_0^{\bar{l}}(t)} dt, \quad (3.14)$$

where we have the same (as in the Statement 1) explicit heteroclinic set (3.12) for the Melnikov function.

3.2. Chaos detection in the dynamical system of the asymmetrical DSSC

3.2.1. The case with Hamiltonian perturbations

Let us consider an example of the motion of the asymmetrical DSSC with the small angular ($\alpha_2 \neq 0, \beta_2 \neq 0$) and linear ($l_{2x} \neq 0, l_{2y} \neq 0$) displacements of the axis of the coaxial bodies rotation (P_1P_2 at the fig.1) relative to the principal central frame $C_2\bar{x}_2\bar{y}_2\bar{z}_2$ of the main-body, and without analogous possible displacements of the rotor-body ($\alpha_1 = \beta_1 = l_{1x} = l_{1y} = 0$) at the action of the magnetic (1.51) and biharmonic (1.59) perturbations, which is fulfilled at this conditions:

$$\begin{cases} e_B \neq 0; e_l \neq 0; e_1 \neq 0; e_m \neq 0; e_\delta \neq 0; \\ \alpha_2 \neq 0, \beta_2 \neq 0; l_{2x} \neq 0, l_{2y} \neq 0; \\ \alpha_1 = \beta_1 = l_{1x} = l_{1y} = 0; \\ c_z = 1; s_z = 0; N = 2 \end{cases} \quad (3.15)$$

Then the Melnikov-Wiggins function will have the form, which follows from (3.14), (1.60), (1.61), and taking into account expressions (1.40) and (1.32):

$$\begin{aligned} M_2^{\bar{I}}(w_0) &= - \int_{-\infty}^{+\infty} \left[\frac{\partial T_1}{\partial \delta} + \frac{\partial P_1^m}{\partial \delta} + \frac{\partial P_1^\delta}{\partial \delta} \right]_{q_0^{\bar{I}}(t)} dt = - \int_{-\infty}^{+\infty} \left[\frac{\partial T_B}{\partial \delta} + \frac{\partial P_1^m}{\partial \delta} + \frac{\partial P_1^\delta}{\partial \delta} \right]_{q_0^{\bar{I}}(t)} dt = \\ &= - \int_{-\infty}^{+\infty} \left[e_B \frac{\bar{A}_1}{2} \left[(\bar{p}^2(t) - \bar{q}^2(t)) \sin(2(\bar{\delta}(t) + w_0)) - \bar{p}(t)\bar{q}(t) \cos(2(\bar{\delta}(t) + w_0)) \right] + \right. \\ &\quad \left. + e_\delta \sum_{n=1}^N n \left(a_n \cos(n(\bar{\delta}(t) + w_0)) - b_n \sin(n(\bar{\delta}(t) + w_0)) \right) - \right. \\ &\quad \left. - e_m \frac{Q}{G} \left(B\bar{q}(t) \cos(\bar{\delta}(t) + w_0) - A\bar{p}(t) \sin(\bar{\delta}(t) + w_0) \right) \right] dt. \end{aligned} \quad (3.16)$$

Using elementary trigonometric transformations, and with the help of the symmetry properties of the odd- and even-functions, we have the following integration result in the form of the trigonometric polynomial:

$$\begin{aligned} M_2^{\bar{I}}(w_0) &= e_B J_B \sin 2w_0 + e_m J_m \sin w_0 + \\ &+ e_\delta \left[J_\delta^{(a_1)} \cos w_0 + J_\delta^{(b_1)} \sin w_0 + J_\delta^{(a_2)} \cos 2w_0 + J_\delta^{(b_2)} \sin 2w_0 \right], \end{aligned} \quad (3.17)$$

where the nonzero constants for the convergent¹ improper integrals take place (we will not reduce the integrals to the explicit analytical expressions):

$$\begin{cases} J_B = - \int_{-\infty}^{+\infty} \frac{\bar{A}_1}{2} \left[(\bar{p}^2(t) - \bar{q}^2(t)) \cos \bar{\delta}(t) + \bar{p}(t)\bar{q}(t) \sin \bar{\delta}(t) \right] dt = \text{const} \neq 0; \\ J_m = \int_{-\infty}^{+\infty} \frac{Q}{G} \left[A\bar{p}(t) \cos \bar{\delta}(t) - B\bar{q}(t) \sin \bar{\delta}(t) \right] dt = \text{const} \neq 0; \\ J_\delta^{(a_1)} = - \int_{-\infty}^{+\infty} a_1 \cos \bar{\delta}(t) dt = \text{const} \neq 0; \quad J_\delta^{(b_1)} = \int_{-\infty}^{+\infty} b_1 \cos \bar{\delta}(t) dt = \text{const} \neq 0; \\ J_\delta^{(a_2)} = -2 \int_{-\infty}^{+\infty} a_2 \cos 2\bar{\delta}(t) dt = \text{const} \neq 0; \quad J_\delta^{(b_2)} = 2 \int_{-\infty}^{+\infty} b_2 \cos 2\bar{\delta}(t) dt = \text{const} \neq 0. \end{cases} \quad (3.18)$$

¹ The convergence of the integrals can be verified numerically and/or analytically.

The Melnikov-Wiggins function in the form of the pure trigonometric polynomial (3.17) with constant coefficients (3.18), obviously, has the infinity set of simple roots, that proves the heteroclinic chaos initiation in the magnetized asymmetry DSSC attitude dynamics at the presence of the considered Hamiltonian perturbations (the constructional asymmetry, magnetic and polyharmonic perturbations). Here it is important to note, that the well-known examples of the homo/heteroclinic chaos initiation in the quite similar Hamiltonian cases were collected in many previous scientific works; e.g. chaos in the free motion of the coaxial rigid bodies systems (the rigid body with attachments) was considered in [Holmes & Marsden (1983)] basing on the Holms'-Marsden's methodology (as the result was obtained the monoharmonic Melnikov function in the form: $M(w_0) = C \sin(2w_0)$); the same monoharmonic result also was presented in the task of a gyrostat motion with asymmetric rotor [Peng (2000)]; also the chaos in the pitch motion of an asymmetric magnetic spacecraft in polar elliptic orbit was studied [Iñarrea (2009)], where the monoharmonic form of the Melnikov function was written; the chaos in the reorientation process of a dual-spin spacecraft with time-dependent moments of inertia was investigated in [Iñarrea (2000)] with obtaining the monoharmonic form of the Melnikov function; the monoharmonic form of the Melnikov function is actual for the chaotic motion of an asymmetric gyrostat in the magnetic field of the Earth at the consideration of the magnetic moment as the small perturbation on the equatorial orbit [Cheng (2000)].

So, now it is worth to present some results of the numerical modeling (fig.5) to show the main properties of the detected chaotic motion. The following system's parameters and initial conditions were taken for the numerical research:

$$\begin{cases} \varepsilon = 0.03; & e_B = e_\delta = 1; & e_l = e_1 = e_m = e_r = 0; \\ a_1 = b_1 = 0, & a_2 = 0.25, & b_2 = -0.9 \text{ [kg} \cdot \text{m}^2 / \text{s}^2]. \end{cases}$$

$$\hat{A}_1 = 5; \quad \bar{C}_1 = 4; \quad \hat{A}_2 = 15; \quad \hat{B}_2 = 10; \quad \bar{C}_2 = 6 \quad \text{[kg} \cdot \text{m}^2];$$

$$\hat{A}_2 = \bar{A}_2 + M_2 \cdot OP_2^2; \quad \hat{B}_2 = \bar{B}_2 + M_2 \cdot OP_2^2.$$

$$p_0 = 1.5, \quad q_0 = 0, \quad r_0 = 1.33124; \quad \sigma_0 = -0.58124 \quad \text{[rad/s];}$$

$$\bar{\Delta} = 3, \quad G = 31.9487 \quad \text{[kg} \cdot \text{m}^2 / \text{s}]; \quad Q = -20, \quad \tilde{T} = 35.8198 \quad \text{[kg} \cdot \text{m}^2 / \text{s}^2].$$

As we can see (fig.5), the complex time-evolutions of the angular velocity components (fig.5-a, -b) and the phase-trajectory in the Serret-Andoyer phase-space (fig.5-d) with the irregular behavior take place. Also in purposes to understand the main properties of the system dynamics, it is very informatively to use the Poincaré sections. The considered in this research Poincaré sections (fig.6) are plotted based on the "stroboscopic" condition, when the corresponding heteroclinic angular phase repeats its own initial value with the 2π -period:

$$[\bar{w}_\delta(t) \bmod 2\pi] = \bar{w}_\delta(0) = 0 \quad (3.19)$$

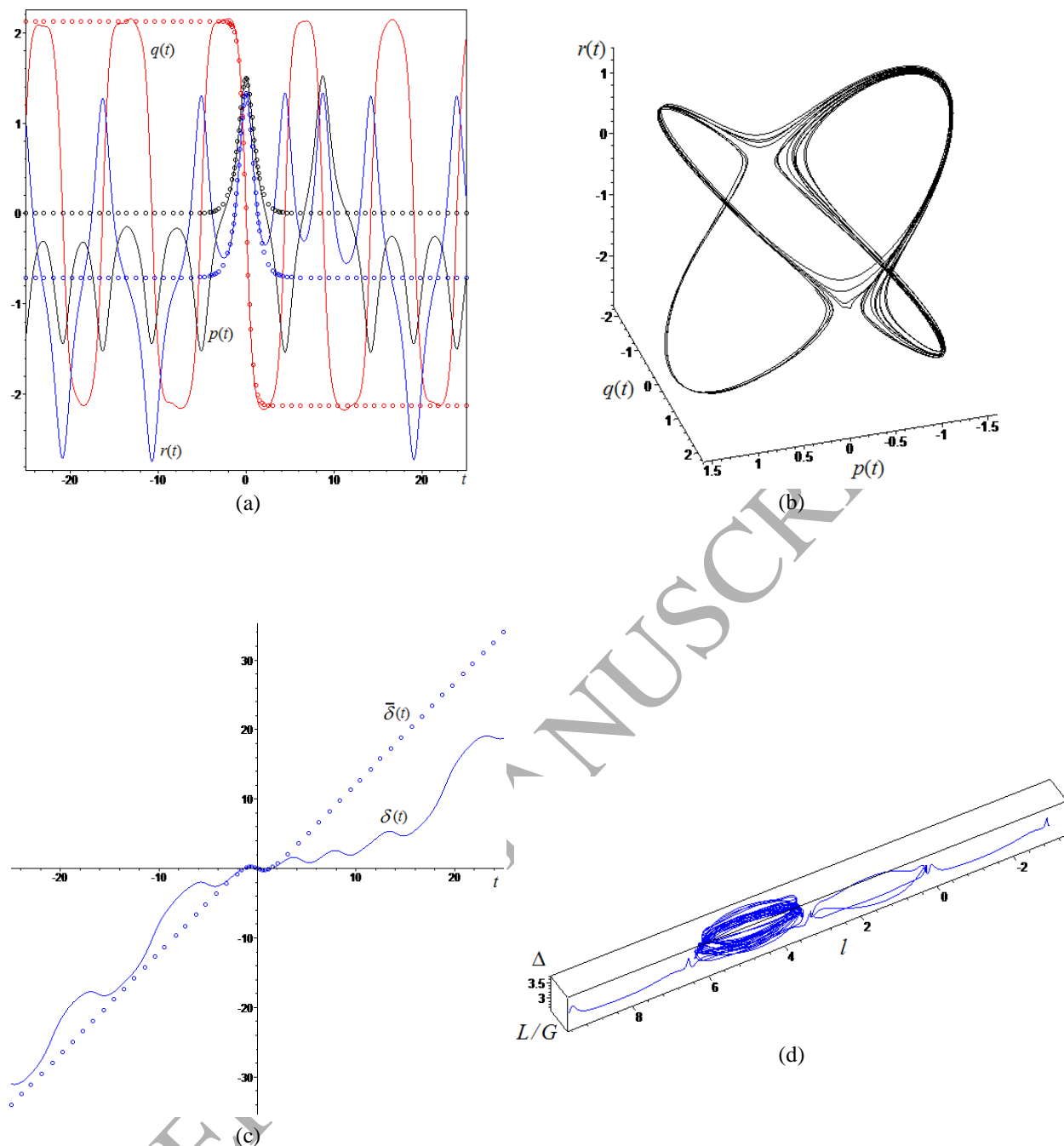


Fig.5. The perturbed angular velocity components and the phase-trajectory near the unperturbed separatrix

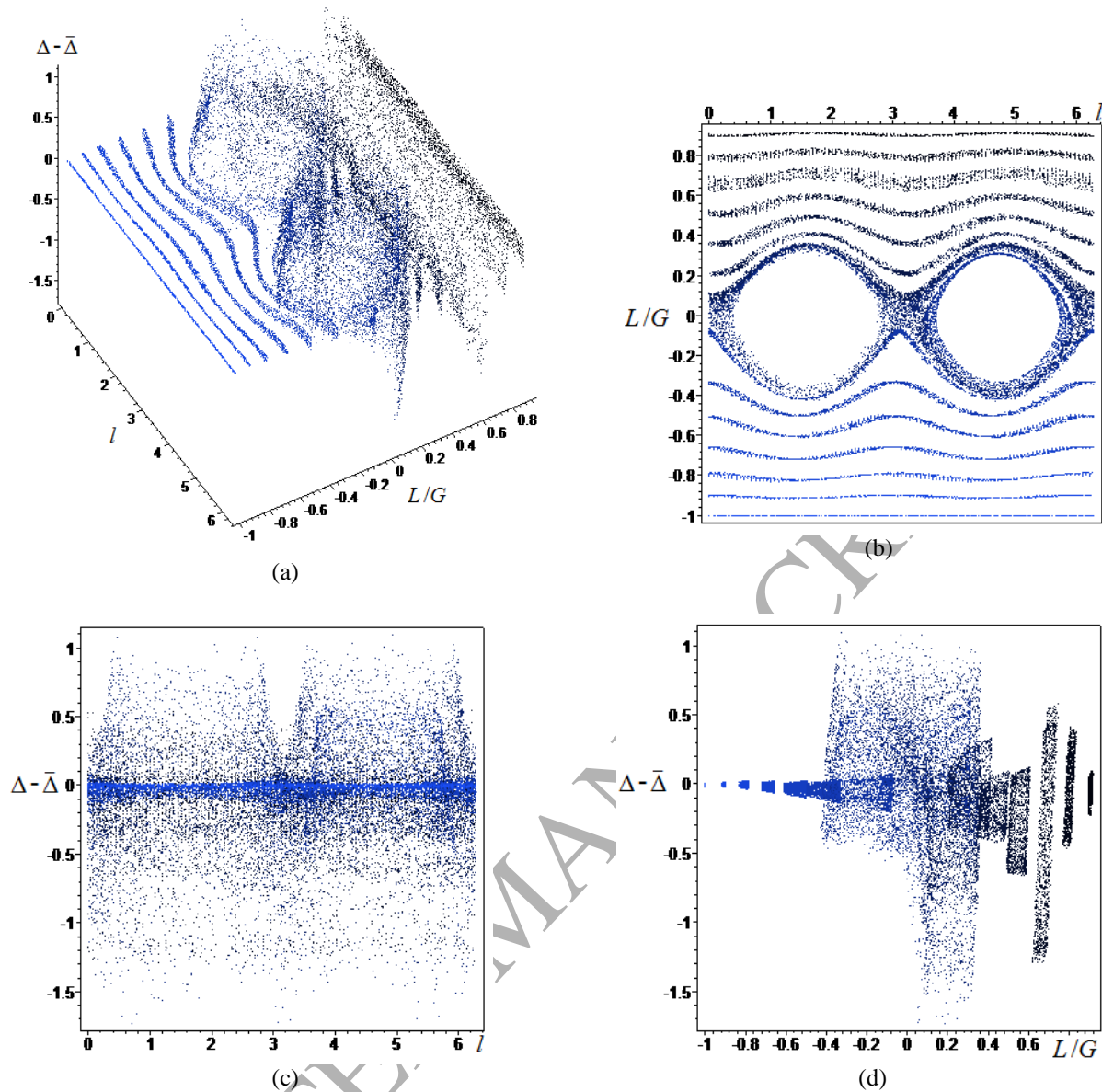


Fig.6. The Poincaré section of the perturbed system's phase space $\{l$ [rad], L/G [dimensionless], $\Delta - \bar{\Delta}$ [kg·m²/s] $\}$:

The color-gradient (from light-blue to black) corresponds to the initial point position from the low-level of the L -momentum ($L/G \approx -1$) to the hi-level of the L -momentum ($L/G \approx 1$) – it shows us to which initial-regions belong to the images of the Poincaré-map

The Poincaré section (fig.6) demonstrates the presence of the heteroclinic chaos close to the separatrix regions, that can be identified as the so-called “chaotic layer” presented the “cloud” of the Poincaré points, which do not belong to the regular phase-curves.

Also it is worth to underline the well-known causes of the “chaotic layer” generation [Poincaré (1899), Arnold (1964), Kozlov (1980), Holms (1990)]: homo/heteroclinic orbits can produce the heteroclinic nets/plexuses as the set of the intersected split stable and unstable manifolds of the original homo/heteroclinic orbit at the action of small perturbations. So, the surrounding phase trajectory are compelled to walk round this complex split intersected set of the subordinate heteroclinic manifolds – this dynamical effect results in the realization of complex tangled phase trajectories, and therefore their corresponding “stroboscopic” Poincaré-

points cover the irregular area of the phase-space, that corresponds to the “chaotic layer”. The indicated split intersected subordinate heteroclinic manifolds can be plotted [Doroshin (2012)] as the sets of the Poincaré-images (in the positive time-direction $t \rightarrow +\infty$) and preimages (in the negative time-direction $t \rightarrow -\infty$) of the of the original heteroclinic orbit. Then this images we can consider as the perturbed forms (in the corresponding sections of the full phase-space) of the unstable manifold of the original heteroclinic orbit; and preimages – as the perturbed forms of its stable manifolds. The described first form of the heteroclinic nets is presented at the fig.7.

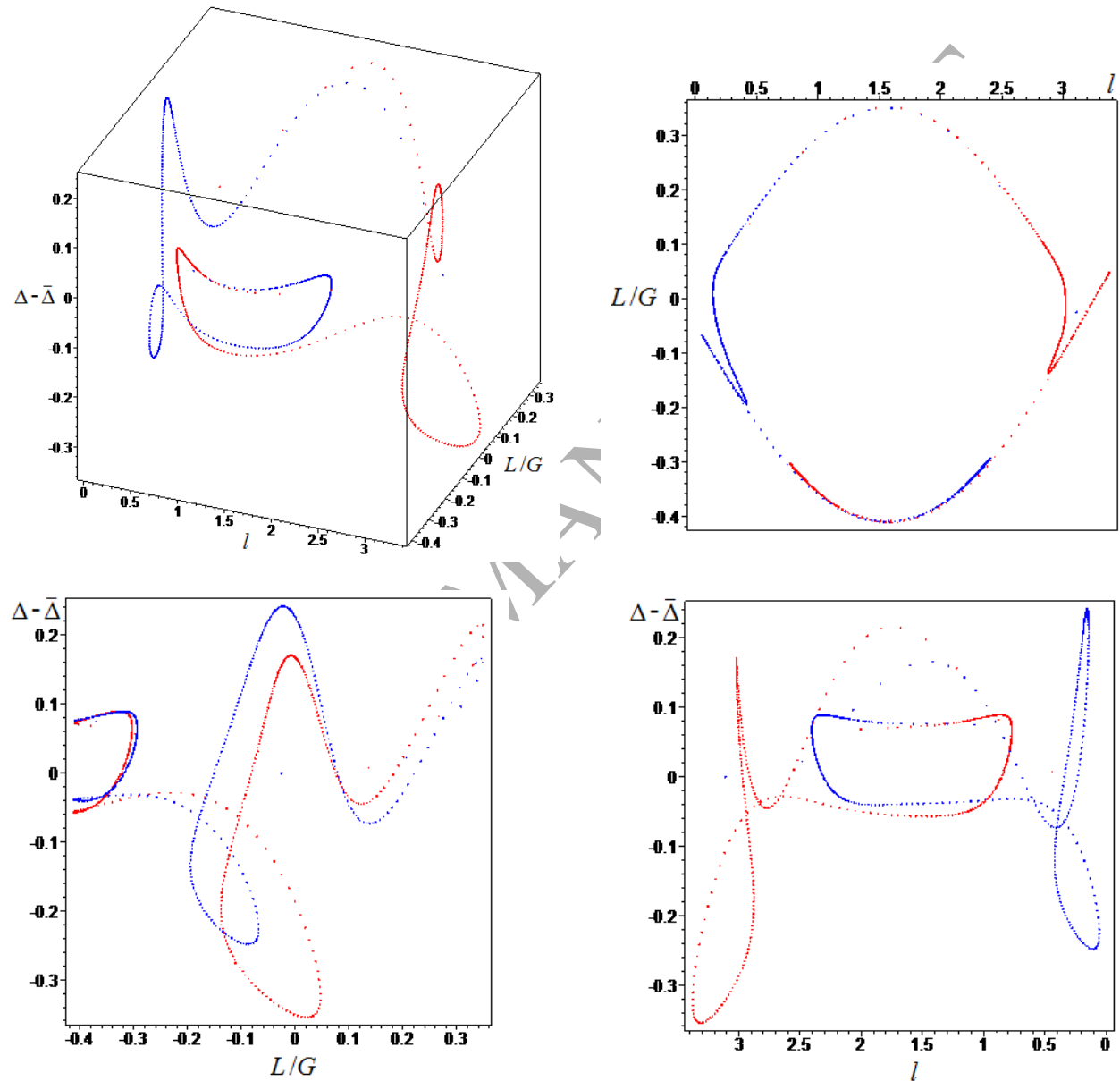


Fig.7. The fragment of the heteroclinic net as the set of the first Poincaré-image (red) and the first Poincaré-preimage (blue) of the unperturbed separatrix

3.2.2. The case with non-Hamiltonian perturbations

Let us now consider the case of the motion of the asymmetrical DSSC under the action of the non-Hamiltonian perturbations, including (1.54) and (1.57). As we can see from the expressions (1.54) and (1.57), the interconnected form of the considering non-Hamiltonian perturbations can

be presented:

$$\begin{cases} m_{\Delta} = m_{\Delta}(\sigma, t) = m_{\Delta}^f + m_{\Delta}^{DC} = -e_{\sigma}\sigma(t) + e_F F(t); \\ F(t) = e_F [\tilde{e}_U U(t) - \tilde{e}_{\kappa} \text{sign}(\sigma(t))]; \\ e_{\sigma} = e_{\nu} + e_{\mu}; \quad e_F = \sup\{e_{\kappa}, e_U\}; \\ \tilde{e}_U = e_U / e_F; \quad \tilde{e}_{\kappa} = e_{\kappa} / e_F \end{cases} \quad (3.20)$$

We can rewrite the expression for the Melnikov-Wiggins function (3.10) in the form with the separation of two parts:

$$M_1^{\bar{I}}(w_0) = M(w_0) + W(w_0), \quad (3.21)$$

where

$$M(w_0) = \int_{-\infty}^{+\infty} [f_i \cdot g_L - f_L \cdot g_i] \Big|_{q_0^{\bar{I}}(t)} dt; \quad (3.22)$$

$$W(w_0) = \int_{-\infty}^{+\infty} (f_{\delta} \Big|_{q_0^{\bar{I}}(t)} - f_{\delta} \Big|_{\gamma(\bar{\Delta})}) \cdot g_{\Delta} \Big|_{q_0^{\bar{I}}(t)} dt \quad (3.23)$$

The function $M(w_0)$ corresponds to the classical Melnikov's function, and the function $W(w_0)$ represents the Wiggins' part. Taking into account the structure (1.63) of the perturbation g_{Δ} it is possible to divide the perturbation on Hamiltonian ($g_{\Delta}^{\mathcal{H}}$) and on non-Hamiltonian ($g_{\Delta}^{\mathcal{NH}}$) parts:

$$g_{\Delta} = g_{\Delta}^{\mathcal{H}} + g_{\Delta}^{\mathcal{NH}}; \quad g_{\Delta}^{\mathcal{H}} = -\frac{\partial \mathcal{H}_1}{\partial \delta}; \quad g_{\Delta}^{\mathcal{NH}} = m_{\Delta}^f + m_{\Delta}^{DC} = m_{\Delta} \quad (3.24)$$

Basing on the expressions (1.63), (1.61) and (1.32), the following form of the right-part-function f_{δ} can be obtained:

$$f_{\delta} = \frac{\partial \mathcal{H}_0}{\partial \Delta} = \frac{(\bar{C}_1 + \bar{C}_2)\Delta - \bar{C}_1 L}{\bar{C}_1 \bar{C}_2} = \bar{\sigma}_0(t);$$

where $\bar{\sigma}_0(t)$ represents the unperturbed time-dependence for the relative rotation angular velocity; therefore, with the help of the heteroclinic solutions (2.1)-(2.4), we can obtain the reduced form of the terms in the parentheses in the expression (3.23):

$$f_{\delta} \Big|_{q_0^{\bar{I}}(t)} = \bar{\sigma}(t); \quad f_{\delta} \Big|_{\gamma(\bar{\Delta})} = f_{\delta} \Big|_{q_0^{\bar{I}}(t \rightarrow \pm\infty)} = \bar{\sigma}(\pm\infty) = \Delta / \bar{C}_1 - (\Delta - EB) / (B - \bar{C}_2) = \sigma_* \quad (3.25)$$

So, the Wiggins' part of the Melnikov-Wiggins function can be rewritten as

$$W(w_0) = W_{\mathcal{H}}(w_0) + W_{\mathcal{NH}} \quad (3.26)$$

where

$$W_{\mathcal{H}}(w_0) = \int_{-\infty}^{+\infty} (\bar{\sigma}(t) - \sigma_*) \cdot g_{\Delta}^{\mathcal{H}} \Big|_{q_0^{\bar{I}}(t)} dt; \quad (3.27)$$

$$W_{\mathcal{NH}} = \int_{-\infty}^{+\infty} (\bar{\sigma}(t) - \sigma_*) \cdot m_{\Delta}(\bar{\sigma}(t), t) dt = J_{\mathcal{NH}} = \text{const} \quad (3.28)$$

Here it is very important to note that the improper integrals (3.27) and (3.28) are guaranteed convergent, because the function $(\bar{\sigma}(t) - \sigma_*)$ is the even-function exponentially damped to zero

at $t \rightarrow \pm\infty$ (it follows from the analytical expressions (2.1)-(2.4), and also it is illustrated at the fig.4). So, the Melnikov-Wiggins function takes the form:

$$M_1^{\bar{l}}(w_0) = M(w_0) + W_{\mathcal{H}}(w_0) + J_{\mathcal{NH}} \quad (3.29)$$

Following further according to the Melnikov-Wiggins formalism, we can obtain auxiliary linking formulas for the terms of the Melnikov-Wiggins function. Basing on the expressions (1.63), (1.61), (1.32) and on the heteroclinic solutions (2.1)-(2.4), it is possible to present the forms of the functions $f_L|_{q_0^{\bar{l}}(t)}$, $f_l|_{q_0^{\bar{l}}(t)}$ which are depended only on time:

$$f_L|_{q_0^{\bar{l}}(t)} = \left(\frac{1}{B} - \frac{1}{A}\right)(G^2 - \bar{L}^2) \sin \bar{l} \cos \bar{l} = AB \left(\frac{1}{B} - \frac{1}{A}\right) \bar{p}(t) \bar{q}(t); \quad (3.30)$$

$$f_l|_{q_0^{\bar{l}}(t)} = -\bar{L} \left(\frac{\sin^2 \bar{l}}{A} + \frac{\cos^2 \bar{l}}{B} \right) + \frac{1}{C_2} (\bar{L} - \bar{\Delta}) = \bar{r}(t) - b(t)(A\bar{p}^2(t) + B\bar{q}^2(t)), \quad (3.31)$$

where

$$b(t) = \frac{\bar{C}_2 \bar{r}(t) + \bar{\Delta}}{G^2 - [\bar{C}_2 \bar{r}(t) + \bar{\Delta}]^2}. \quad (3.32)$$

From the last formulas and from the heteroclinic solutions (2.1)-(2.4) we easy conclude that $f_L|_{q_0^{\bar{l}}(t)}$ is the odd-function, and $f_l|_{q_0^{\bar{l}}(t)}$ is the even-function ($b(t)$ also is the even-function).

For the purpose of expressing the functions $M(w_0)$ and $W_{\mathcal{H}}(w_0)$ in the explicit form, which is depended only on the w_0 -argument, we need to rewrite the expressions for the functions g_L , g_l , $g_{\Delta}^{\mathcal{H}}$ (defined by (1.63) and (3.24) after substituting of the arguments $q_0^{\bar{l}}(t)$ (3.12) with the explicit extraction of the w_0 -harmonic multipliers. This procedure is quite simple, because it requires the implementation of usual trigonometric transformations with reductions of similar terms. Let us here write the results of the indicated procedure in the general shape², collected all of the possible considering cases:

$$\begin{cases} g_L|_{q_0^{\bar{l}}(t)} = \sum_{n=1}^2 (C_{L,n}(t) \cos(nw_0) + S_{L,n}(t) \sin(nw_0)) + C_{L,0}(t); \\ g_l|_{q_0^{\bar{l}}(t)} = \sum_{n=1}^2 (C_{l,n}(t) \cos(nw_0) + S_{l,n}(t) \sin(nw_0)) + C_{l,0}(t); \\ g_{\Delta}^{\mathcal{H}}|_{q_0^{\bar{l}}(t)} = \sum_{n=1}^N (C_{\Delta,n}(t) \cos(nw_0) + S_{\Delta,n}(t) \sin(nw_0)) + C_{\Delta,0}(t); \end{cases} \quad (3.33)$$

where

$$\begin{cases} C_{i,n}(t) = C_{i,n}(\bar{L}(t), \bar{l}(t), \bar{\delta}(t)) = C_{i,n}(\bar{p}(t), \bar{q}(t), \bar{r}(t), \bar{\delta}(t)); & n = 0 \dots N; \\ S_{i,n}(t) = S_{i,n}(\bar{L}(t), \bar{l}(t), \bar{\delta}(t)) = S_{i,n}(\bar{p}(t), \bar{q}(t), \bar{r}(t), \bar{\delta}(t)); & i = \{L, l, \Delta\} \end{cases} \quad (3.34)$$

The substitution of the functions (3.30)-(3.33) into the integrals (3.22), (3.27) and improper integration using the symmetry properties of the odd- and even-functions gives us the general trigonometric polynomial form of the Melnikov-Wiggins function:

$$M_1^{\bar{l}}(w_0) = P_{\text{trig}}(w_0) + J_{\mathcal{NH}}; \quad (3.35)$$

² The possible explicit form of the functions (3.33) we will present below in the framework of an example in the section 3.3.

where

$$P_{trig}(w_0) = M(w_0) + W_{\mathcal{H}}(w_0) = \sum_{n=0}^N (J_{c,n} \cos(nw_0) + J_{s,n} \sin(nw_0)); \quad J_{c,n} = \text{const}; \quad J_{s,n} = \text{const} \quad (3.36)$$

Constants $J_{s,n}$ and $J_{c,n}$ are defined by concrete forms of the expressions (3.33) and by the corresponding results of the improper integrations³ (some of integrals, certainly, will be equal to zero).

It is worth to remark that the form (3.35) of the Melnikov-Wiggins function can be characterized as the generalized form collecting all types of the natural perturbations considering in this research (i.e. asymmetrical, external magnetic, internal electromagnetic perturbations, the internal friction, and polyharmonic signals of the control systems); and, therefore, basing on the Melnikov-Wiggins formalism this form describes the possibility of the realization of the chaotic/regular motion modes of the magnetized asymmetrical DSSC in the considered general case. Here we could note, that the comparative analysis of the result (3.35) relative the previous well-known results [Holmes & Marsden (1983); Iñarrea & Lanchares, V. (2000); Iñarrea (2003); Iñarrea, Lanchares at al. (2003); Kuang (2001), (2006); Leung (2004); Baozeng (2007); Bao-Zeng (2008); Or (1998)] is presented in the next section of this paper.

So, as the local conclusion we can underline the simple polyharmonic structure of the Melnikov-Wiggins function (3.35), which implies the uncountable set of simple roots – this circumstance formally proves in the general case the presence of the heteroclinic chaos in the system dynamics. The presence of the heteroclinic chaos in the asymmetrical DSSC/gyrostat dynamics is well known fact, which was investigated in different formulations in many works. Therefore, here it is needed to give some comments about the new providing in this work research in the comparison with the known previous tasks:

1. Firstly, in this research the general and most complete constructional and mass-inertia asymmetry of the DSSC (fig.1) is considered. The corresponding mechanical and mathematical models are constructed, including the Hamiltonian form and important conjunctive expressions for all types of perturbations.
2. Secondly, the case of the motion of the magnetized DSSC in the constant magnetic field (it corresponds to the equatorial circle orbits of the Earth/planets) at the implementation of the important regime of the cylindrical precession is investigated. The new corresponding heteroclinic solutions [Doroshin (2015)] are used for the investigation of the chaotic aspects – these solutions generalize the analogous heteroclinic solutions for the free DSSC/gyrostats.
3. In the considering case, the heteroclinic action-angle variables for the rotational phase are obtained in the exact analytical form. These heteroclinic action-angle variables allow the correct application of the Melnikov's-Wiggins' formalism; as the result the simple general analytical polyharmonic form of the Melnikov function was found.
4. In the contrast to the previous works, in this research the real natural forces and torques are considered, including the friction between the coaxial DSSC bodies, electromotor's

³ The convergence of the integrals can be proved by numerical and/or analytical calculations (an example will be given below in the next section of the article).

torques applied to the rotor from the platform by internal engines, the counterelectromotive force/torques in such internal engines due to the rotor's rotation, internal plyharmonic and external magnetic perturbations. All of them are the natural instruments of the motion parameters changing and the chaos control/avoidance.

3.3. The heteroclinic chaos suppression in the DSSC dynamics

Let us investigate the possibility of the suppression/control of the heteroclinic chaos in the perturbed DSSC system. First of all, we must define the “natural toolkit” which in principal can affect the heteroclinic chaos characteristics (e.g. the maximal amplitude of the chaotic oscillations, the location of the area of the chaotic dynamics in the phase space, the thickness of the chaotic layer, and, ultimately, the presence/avoidance of chaos). Certainly, only controlled forces/torques and DSSC parameters can be selected on the roles of regularizing factors suppressing the chaos. Therefore, some specific set of internal torques (the corresponding coefficients which are available to change at the preparation of space missions) and DSSC parameters (kinematical, dynamical, mass-inertial, geometrical and other) are useful for the chaos control. So, below we try to apply these instruments to the chaos possible suppression, considering two main cases: the Hamiltonian case of perturbations, and the non-Hamiltonian one.

In the case with Hamiltonian perturbations we have the Melnikov-Wiggins function (3.17) which represents the pure trigonometric polynomial without any free terms (additional constants) – this fact provides the presence of simple roots of the Melnikov-Wiggins function in any considered case of the Hamiltonian perturbations and parameters of the DSSC motion. Hence, the elimination of the heteroclinic chaos in the considered cases with Hamiltonian perturbations is impossible – at least, it follows from the results of the Wiggins formalism application to the considered heteroclinic task.

Now we describe the cases of the asymmetrical DSSC attitude motion at the action of the non-Hamiltonian perturbations. Applying the trigonometric polynomial form (3.35) of the Melnikov-Wiggins function, we can conclude that the condition of the absence of its simple roots can be written as the inequality

$$Am(P_{irig}(w_0)) \leq |J_{\mathcal{NH}}| \quad (3.37)$$

where the function $Am(\bullet)$ means the estimation of the amplitude of the trigonometric polynomial (as the maximum positive value on the corresponding period). Here it is worth to note that the condition (3.37) provides the shift of the graph of the trigonometric polynomial $P_{irig}(w_0)$ along the ordinate-direction, and the roots are vanished. There is no difference between the shift directions (it can be fulfilled up or down the ordinate) and, hence, the sign of the constant $J_{\mathcal{NH}}$ is not important. Thus the inequality (3.37) is represents the condition of the heteroclinic chaos suppression and also defines the system “critical” parameters (constructional, kinematical, dynamical etc.) which “disable” the heteroclinic chaos.

The similar conditions for other cases of the DSSC motion also are known [Iñarrea (2003); Iñarrea & Lanchares, V. (2000); Kuang (2001), (2006); Leung (2004); Baozeng (2007); Bao-Zeng (2008); Or (1998)]. Here we have to say, firstly, that basing on the Melnikov-Wiggins formalism the chaos suppressing condition, analogous to the expression (3.37), was obtained in the paper [Kuang (2001)] at the consideration of the task of the asymmetrical gyrostats attitude motion under the action of external dissipative torques and monoharmonic perturbations – the

chaos suppressing condition [Kuang (2001)] represents the particular case of the generalizing formula (3.37) and corresponds to the monoharmonic form ($N=1$) of the trigonometric polynomial (3.36). Secondly, the similar monoharmonic condition was obtained based on the Melnikov-Wiggins formalism in [Iñarra M., Lanchares V., Rothos V. M., Salas J. P. (2003)] where the harmonic variability of the inertia moments and the external dissipative torque were considered. Related monoharmonic conditions are appeared among the research results in works [Kuang (2006); Leung (2004), (2007)] where the perturbed system are investigated with the help of the Melnikov–Holmes–Marsden (MHM) integrals [Holmes & Marsden (1983)]. Criteria of chaotic rotations in the monoharmonic form were formulated by means of the classical Melnikov integral in works [Iñarra & Lanchares (2000); Baozeng (2007); Bao-Zeng (2008); Or (1998)]. Also it is possible to mention the aspiration [Aslanov & Yuditsev (2012), (2014)] to the fulfillment of the analysis of the asymmetric DSSC chaotic motion with the synthesis of corresponding chaos suppressing conditions, but here we have to state, that the Melnikov’s-Wiggins’ formalism in these works [Aslanov, Yuditsev (2012), (2014)] was used incorrectly – this circumstance invalidates the corresponding published results.

So, we can locally conclude that the above mentioned form of the suppressing condition is quite useful in the research of the space flight dynamics – this monoharmonic form is the particular case of the generalized polyharmonic form (3.37) of the chaos suppressing condition, obtained in this work. Now let us give examples of the chaos suppressing techniques, which are based on the general condition (3.37).

The dissipative technique of the heteroclinic chaos suppressing. In purposes of the illustration of the obtained general results and conditions let us analytically consider an example of the asymmetrical magnetized DSSC dynamics with the non-Hamiltonian perturbation at the following values of the perturbation’s parameters:

$$e_B \neq 0; e_m \neq 0; e_\sigma \neq 0; c_\chi = 1; e_l = e_1 = e_\delta = e_r = 0; s_\chi = 0. \quad (3.38)$$

Then after elementary transformations the following coefficients (3.34) can be written taking into account assumptions (3.38), basing on expressions (1.63), (1.32) and substituting the heteroclinic solutions:

$$\begin{cases} C_{L,1}(t) = e_m \frac{Q}{G} [B\bar{q}(t) \cos \bar{\delta}(t) - A\bar{p}(t) \sin \bar{\delta}(t)]; \\ S_{L,1}(t) = -e_m \frac{Q}{G} (B\bar{q}(t) \sin \bar{\delta}(t) + A\bar{p}(t) \cos \bar{\delta}(t)); \\ C_{L,2}(t) = \frac{e_B \bar{A}_1}{2AB} [(B^2 \bar{q}^2(t) - A^2 \bar{p}^2(t)) \sin 2\bar{\delta}(t) + (A^2 + B^2) \bar{p}(t) \bar{q}(t) \cos 2\bar{\delta}(t)]; \\ S_{L,2}(t) = -\frac{e_B \bar{A}_1}{2AB} ((A^2 + B^2) \bar{p}(t) \bar{q}(t) \sin 2\bar{\delta}(t) + (A^2 \bar{p}^2(t) - B^2 \bar{q}^2(t)) \cos 2\bar{\delta}(t)); \end{cases} \quad (3.39)$$

$$\begin{cases} C_{l,1} = e_m \frac{Q}{G} b(t) [B\bar{q}(t) \sin \bar{\delta}(t) + A\bar{p}(t) \cos \bar{\delta}(t)]; \\ S_{l,1} = e_m \frac{Q}{G} b(t) (B\bar{q}(t) \cos \bar{\delta}(t) - A\bar{p}(t) \sin \bar{\delta}(t)); \\ C_{l,2}(t) = e_B \bar{A}_1 \frac{b(t)}{2} [(\bar{p}^2(t) - \bar{q}^2(t)) \cos 2\bar{\delta}(t) + 2\bar{p}(t)\bar{q}(t) \sin 2\bar{\delta}(t)]; \\ S_{l,2}(t) = -e_B \bar{A}_1 \frac{b(t)}{2} ((\bar{p}^2(t) - \bar{q}^2(t)) \sin 2\bar{\delta}(t) - 2\bar{p}(t)\bar{q}(t) \cos 2\bar{\delta}(t)); \end{cases} \quad (3.40)$$

$$\begin{cases} C_{\Delta,1} = e_m \frac{Q}{G} [B\bar{q}(t) \cos \bar{\delta}(t) - A\bar{p}(t) \sin \bar{\delta}(t)]; \\ S_{\Delta,1} = -e_m \frac{Q}{G} (B\bar{q}(t) \sin \bar{\delta}(t) + A\bar{p}(t) \cos \bar{\delta}(t)); \\ C_{\Delta,2}(t) = -e_B \bar{A}_1 \frac{1}{2} [(\bar{p}^2(t) - \bar{q}^2(t)) \sin 2\bar{\delta}(t) - 2\bar{p}(t)\bar{q}(t) \cos 2\bar{\delta}(t)]; \\ S_{\Delta,2}(t) = -e_B \bar{A}_1 \frac{1}{2} ((\bar{p}^2(t) - \bar{q}^2(t)) \cos 2\bar{\delta}(t) + 2\bar{p}(t)\bar{q}(t) \sin 2\bar{\delta}(t)); \end{cases} \quad (3.41)$$

$$\begin{cases} C_{L,0}(t) = \frac{e_B \bar{A}_1}{2AB} [(A^2 - B^2) \bar{p}(t)\bar{q}(t)]; \\ C_{l,0}(t) = -e_B \bar{A}_1 \frac{b(t)}{2} [\bar{p}^2(t) - \bar{q}^2(t)]; \\ C_{\Delta,0}(t) = 0; \end{cases} \quad (3.42)$$

Indicated groups of the explicit coefficients (3.39)-(3.42) make it possible to fulfill the integration and to write the following amplitudes for the harmonics of the trigonometric polynomial (3.36), which corresponds to the Hamiltonian part of the Melnikov-Wiggins function (here we use the properties of odd and even functions, so the terms from (3.39)-(3.42) in square brackets give the zero-result at the improper integration):

$$\begin{cases} J_{c,i} = \int_{-\infty}^{+\infty} ([f_l(t) \cdot C_{L,i}(t)] - [f_L(t) \cdot C_{l,i}(t)] + [(\bar{\sigma}(t) - \sigma_*) C_{\Delta,i}(t)]) dt = 0; \\ J_{s,i} = \int_{-\infty}^{+\infty} (f_l(t) \cdot S_{L,i}(t) - f_L(t) \cdot S_{l,i}(t) + (\bar{\sigma}(t) - \sigma_*) S_{\Delta,i}(t)) dt = \text{const} \neq 0 \end{cases} \quad (3.43)$$

As the result, the biharmonic form of the trigonometric polynomial (3.36) is followed, where we can explicitly select the parts, corresponding to the types of the small perturbations (indicating with multipliers e_m and e_B):

$$P_{\text{irrig}}(w_0) = e_m \bar{J}_{s,1} \sin(w_0) + e_B \bar{J}_{s,2} \sin(2w_0); \quad (\bar{J}_{s,1} = J_{s,1} / e_m; \quad \bar{J}_{s,2} = J_{s,2} / e_B) \quad (3.44)$$

The non-Hamiltonian part of the Melnikov-Wiggins function in the considering case is formed by the small dissipative internal interaction (including the liquid-type friction and the torque from the counterelectromotive force):

$$m_{\Delta} = -e_{\sigma} \sigma(t) \quad (3.45)$$

The corresponding integral (3.28) takes the form:

$$J_{\mathcal{NH}} = e_\sigma \bar{J}_{\mathcal{NH}}; \quad \bar{J}_{\mathcal{NH}} = - \int_{-\infty}^{+\infty} (\bar{\sigma}(t) - \sigma_*) \bar{\sigma}(t) dt = \text{const} \quad (3.46)$$

So, basing on the condition (3.37), the expressions (3.44) and (3.46) compose the chaos suppression criterion. Also from the condition (3.37) the “critical” value of the dissipation follows as the value of the coefficient e_σ which corresponds to the fulfilment of the limiting equality in the unstrict inequality (3.37):

$$\bar{e}_\sigma = \frac{Am(P_{\text{trig}}(w_0))}{|\bar{J}_{\mathcal{NH}}|} \quad (3.47)$$

At the critical dissipation value (3.47) we have the suppression of the heteroclinic chaos as the implementation of the separatrix splitting without intersections of stable and unstable manifolds of the heteroclinic orbit. Certainly, we did not obtain here the final analytic representations for the integrals (it can be provided in the separated research), but we wrote them in the closed form, that allows to provide the clear numerical simulation of the chaotic properties of the asymmetrical DSSC in the considering case.

Let us show some numerical results for the magnetized asymmetrical DSSC dynamics simulation with the formulation of possible suggestions for the practical application.

Beforehand, we should note that the phase portrait contains two main heteroclinic orbits (the “upper” and the “lower” separatrix in the Serret-Andoyer phase-space) at the same system’s angular momentum (G) and energy level (\tilde{T}) of the saddle-points. These two separatrices fully correspond to the heteroclinic solutions (2.1)-(2.6) and to two sets of the initial conditions for the two heteroclinic polhodes on the ellipsoid of the angular momentum [Doroshin (2012), (2013b), (2015)].

So, now we numerically consider the case of the asymmetrical DSSC motion at the action of the perturbations with the following coefficients:

$$\varepsilon = 0.15; \quad e_B = 1; \quad e_\sigma \neq 0; \quad e_l = e_1 = e_\delta = e_m = e_F = 0.$$

The DSSC inertia-mass parameters are:

$$\begin{aligned} \hat{A}_1 = 5; \quad \bar{C}_1 = 4; \quad \hat{A}_2 = 15; \quad \hat{B}_2 = 10; \quad \bar{C}_2 = 6 \quad [\text{kg} \cdot \text{m}^2]; \\ \hat{A}_2 = \bar{A}_2 + M_2 \cdot OP_2^2; \quad \hat{B}_2 = \bar{B}_2 + M_2 \cdot OP_2^2 \end{aligned} \quad (3.48)$$

The motion initial conditions for the upper separatrix are:

$$\begin{cases} p_0 = 1.5; \quad q_0 = 0; \quad r_0 = 3.15597; \quad \sigma_0 = 0.59403; \quad \sigma_* = 2.63527 \quad [\text{rad/s}]; \\ \bar{\Delta} = 15; \quad G = 45.29504 \quad [\text{kg} \cdot \text{m}^2/\text{s}]; \quad Q = -15, \quad \tilde{T} = 91.74372 \quad [\text{kg} \cdot \text{m}^2/\text{s}^2], \end{cases} \quad (3.49)$$

and for the lower separatrix:

$$\begin{cases} p_0 = 2.25894; \quad q_0 = 0; \quad r_0 = -1.95929; \quad \sigma_0 = 5.70929; \quad \sigma_* = 2.63527 \quad [\text{rad/s}]; \\ \bar{\Delta} = 15; \quad G = 45.29504 \quad [\text{kg} \cdot \text{m}^2/\text{s}]; \quad Q = -15, \quad \tilde{T} = 91.74372 \quad [\text{kg} \cdot \text{m}^2/\text{s}^2]. \end{cases} \quad (3.50)$$

Firstly we present the numerical results of the motion modelling without the internal dissipation ($e_\sigma = 0$). As can we see at the corresponding figures (fig.8-10), the complex behavior of the system takes place, that shows the chaotic properties of the dynamics, including aperiodic oscillations (fig.8-a) and the complex phase trajectories (fig.8-b-d) which “tie themselves in

knots” [Holms P. J. (1990)]; also we see the chaotic layer (fig.9), and the heteroclinic net (the reciprocal intersections of stable and unstable manifolds of the pair of heteroclinic separatrices – fig.10).

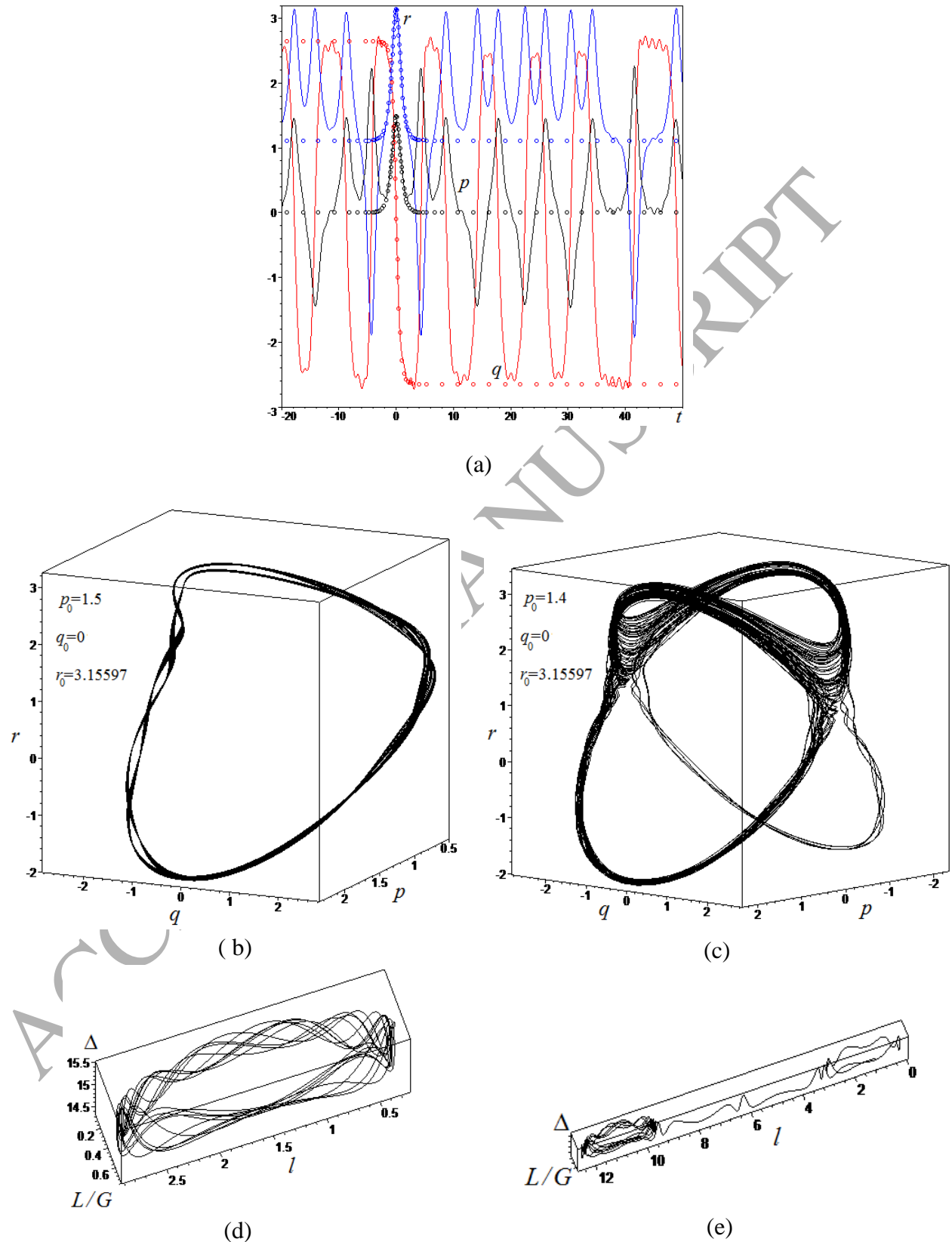


Fig. 8. The angular velocity and the phase-trajectories of the system close to the unperturbed separatrix:
 (a) – the angular velocity components (dots – heteroclinic solutions, lines – perturbed solutions);
 (b), (c) – the polhodes in the p - q - r 3D-phase-space of the angular velocity components;

(d), (e) – the corresponding phase-trajectories in the Serret-Andoyer phase-space

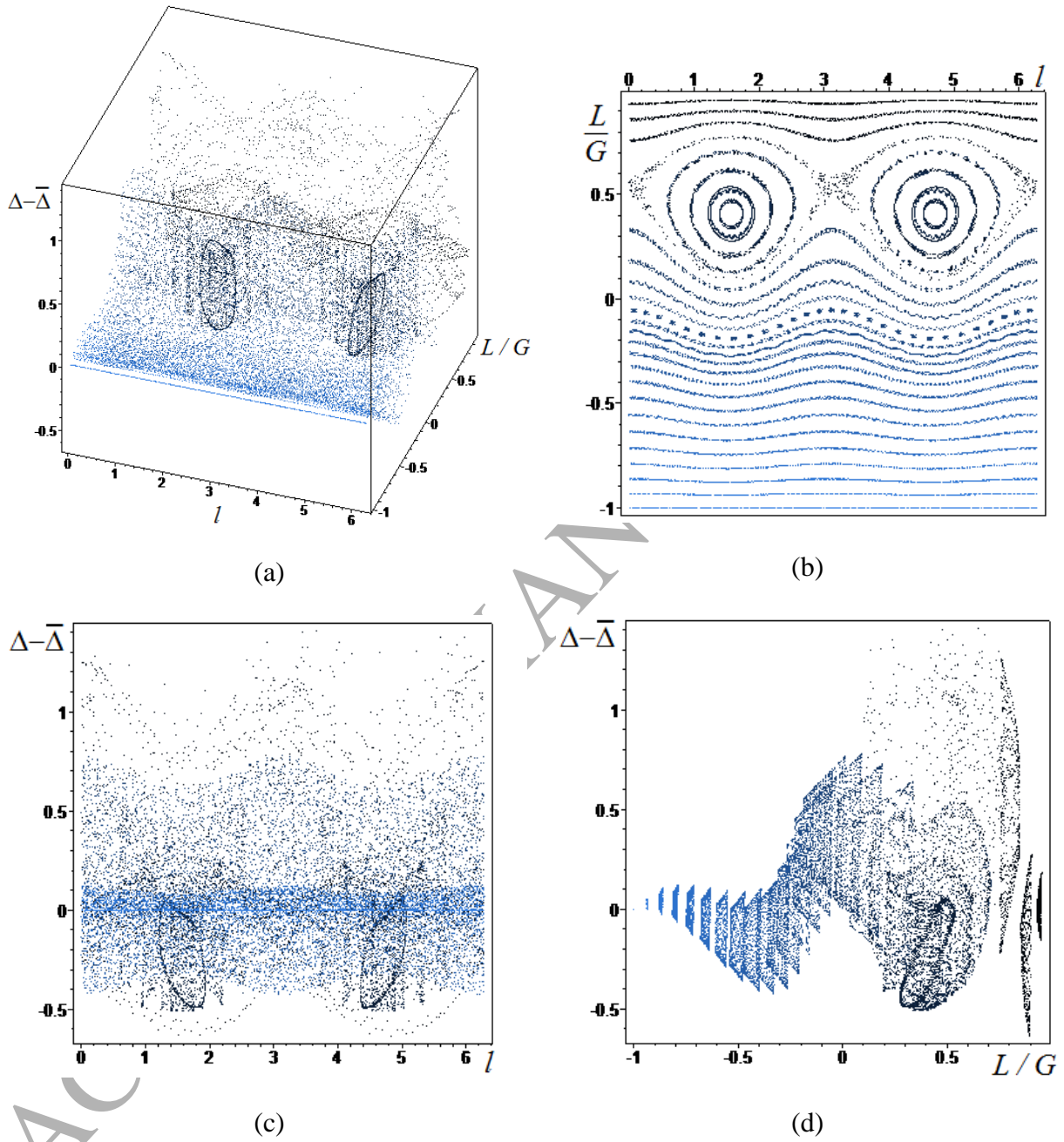


Fig.9. The Poincaré section of the perturbed system's phase space ($m_{\Lambda} = 0$)
 $\{l \text{ [rad]}, L/G \text{ [dimensionless]}, (\Delta - \bar{\Delta}) \text{ [kg} \cdot \text{m}^2/\text{s}]\}$

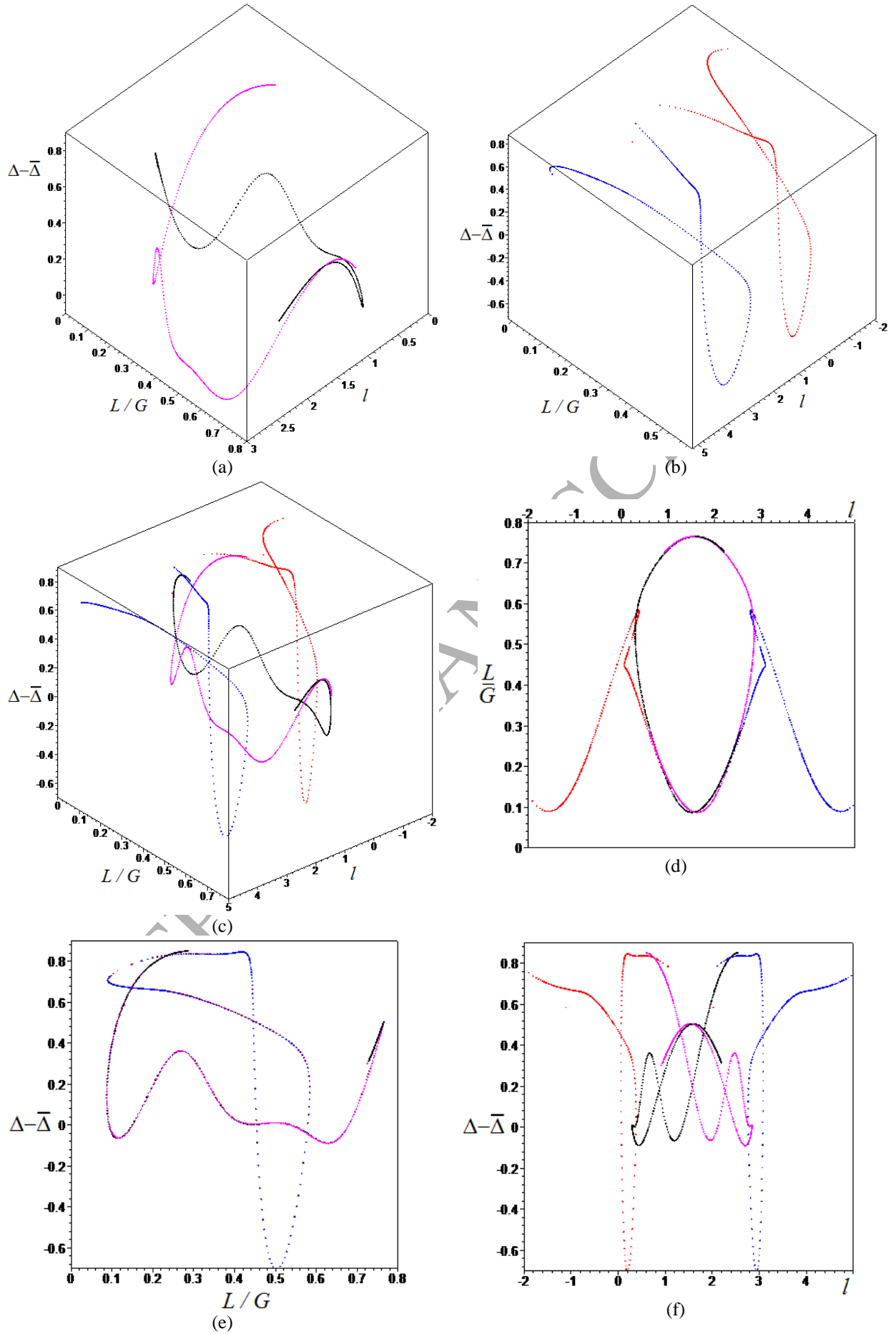


Fig.10. The first Poincaré-images (magenta, red) and the first Poincaré-preimages (black, blue) of the unperturbed heteroclinic separatrices (upper, lower)

Now we present the motion modelling results at the action of the dissipative torque (3.45) in the case of the critical dissipation. It is quite understandable, that at the presence of the pair of the heteroclinic orbits, the resulting critical dissipation is defined by the supremum of the critical coefficients \bar{e}_σ (3.47) separately calculated for the upper separatrix (\bar{e}_σ^{up}) and for the lower separatrix (\bar{e}_σ^{low}):

$$\bar{e}_\sigma = \sup\{\bar{e}_\sigma^{up}, \bar{e}_\sigma^{low}\} \quad (3.51)$$

So, we have $\bar{e}_\sigma^{up} = 0.623313$; $\bar{e}_\sigma^{low} = 0.000219$; $\bar{e}_\sigma = 0.623313$.

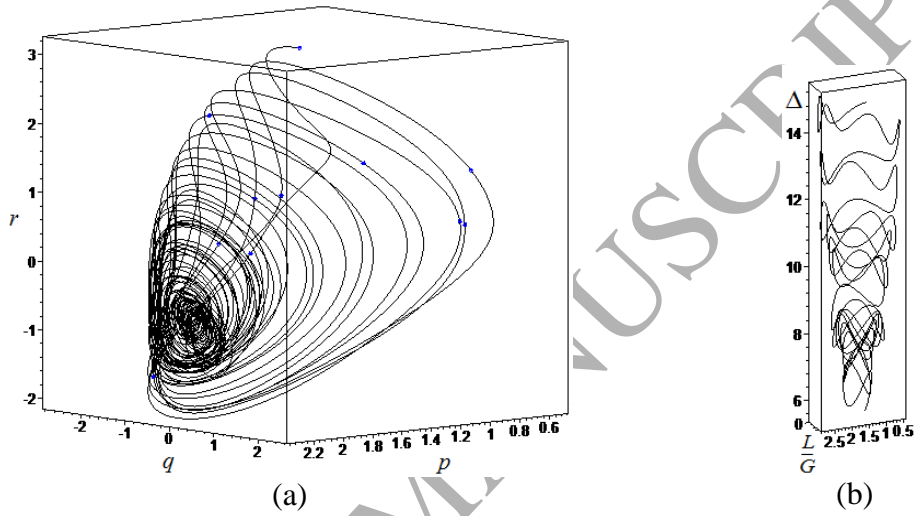


Fig. 11. The phase-trajectory close to the upper separatrix (at the critical \bar{e}_σ):
 (a) – the polhode in the p - q - r 3D-phase-space of the angular velocity components
 (b) – the phase-trajectory in the Serret-Andoyer phase-space

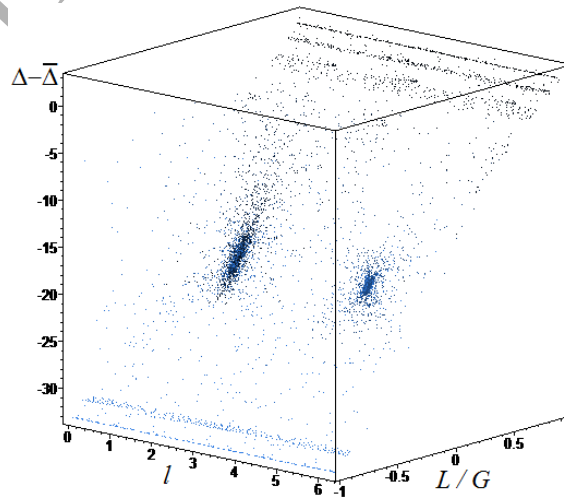


Fig. 12. The Poincaré section of the perturbed system's phase space (at the critical \bar{e}_σ)
 $\{l [\text{rad}], L/G [\text{dimensionless}], (\Delta - \bar{\Delta}) [\text{kg} \cdot \text{m}^2/\text{s}]\}$

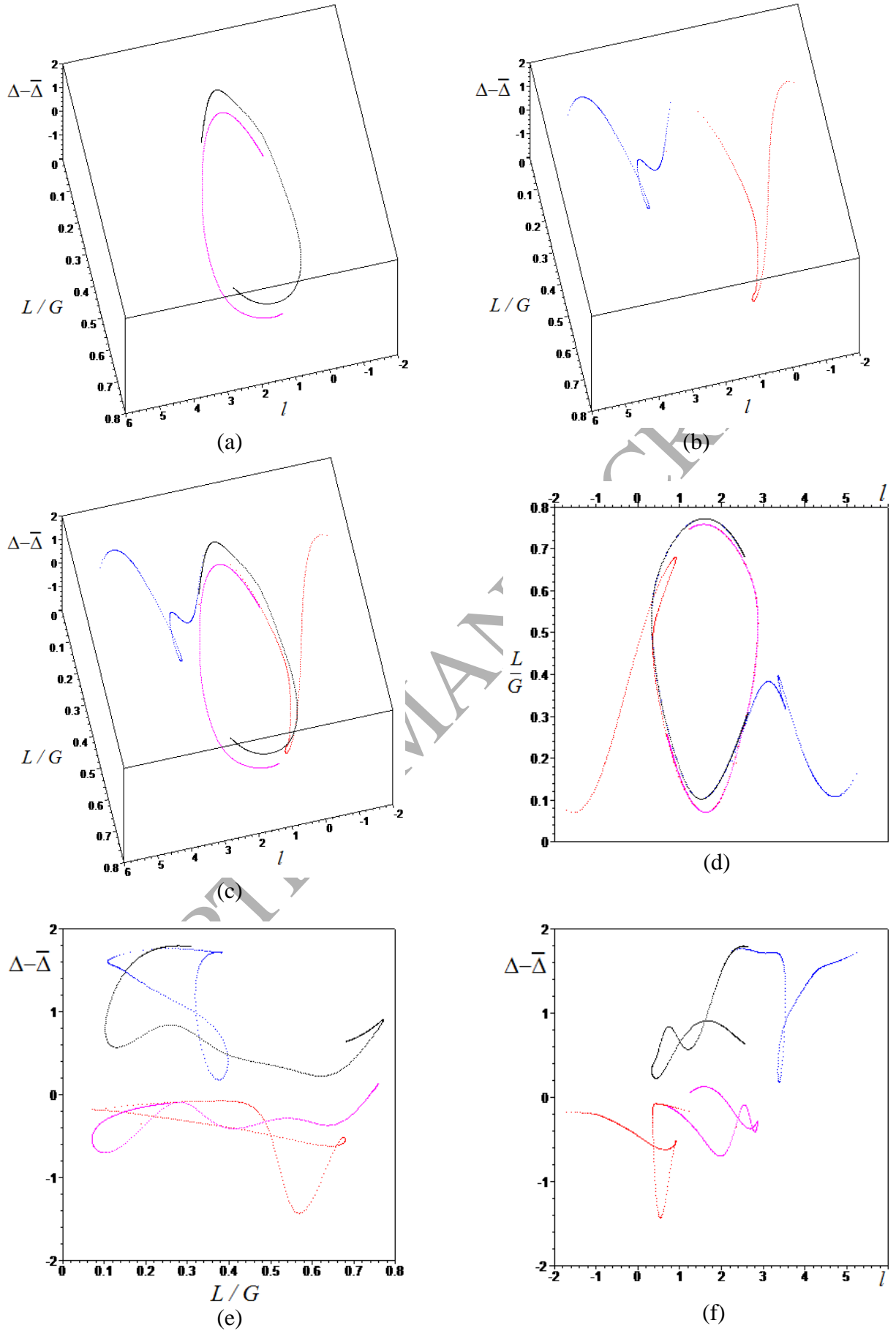


Fig. 13. The heteroclinic net fragment as the set of the first Poincaré-images (magenta, red) and the first Poincaré-pre-images (black, blue) of the unperturbed separatrices (upper, lower) at the critical \bar{e}_σ

As can we see from the numerical modelling results (fig.11-13), the regularization of the original chaotic motion regime (without suppressing torques it was chaotic (fig.8-10)) is implemented in the sense of the dissipative trend in the dynamics: we see the twisted up polhode (fig.11-a), damped oscillations in the Serret-Andoyer phase space (fig.11-b), and the “concentrated” Poincaré mapping (fig.12).

The most interesting aspect of the motion regularization is presented at the (fig.13), where we can observe the separation of manifolds of the heteroclinic trajectory without reciprocal intersections; e.g. at the frame (fig.13-a) we see splitting the “upper” separatrix into nonintersecting manifolds (magenta and black curves), and at the frame (fig.13-b) the analogous nonintersecting separation of the “lower” separatrix is shown (red and blue curves). So, this is the main demonstration and the confirmation of the local chaos suppression, which is implemented with the help of the natural forces/torques (the internal coaxial-bodies-system friction, electromotor’s torques, counterelectromotive forces/torques) – there are no intersections between the split manifolds of the heteroclinic trajectory. But, we should note at the same time, that the intersections of split manifolds belonging to different heteroclinic trajectories are possible: as can we see (fig.13-c-f), the intersections of perturbed stable manifolds (black and blue curves) of the upper and lower separatrices, and also the intersections of perturbed unstable manifolds (magenta and red curves) are available. This circumstance, in fact, means the presence of the heteroclinic net in the global scale at the realized local heteroclinic chaos suppression in the Melnikov-Wiggins sense (concerning nonintersecting split manifolds of one single heteroclinic trajectory/orbit).

Also one actual dynamical task here can be formulated – it is the task of finding such dynamical conditions, which are “neutral/insensitive” to the chaos suppressing in the indicated Melnikov-Wiggins sense at the action of sufficiently large dissipative torque. It means the nonoperability of this chaos suppressing technique. As it follows from the above considered case with the dissipative torque (3.45), the main heteroclinic chaos suppression is fulfilled through the constant part of the Melnikov-Wiggins function generated by the integral (3.46). This integral can take the zero-value at some parameters of the system, and in such cases basing on the Melnikov-Wiggins methodology the heteroclinic chaos suppression is impossible, because the simple roots of the Melnikov-Wiggins function are not vanished. The corresponding system’s parameters can be indicated as the “insensitive” to the influence of the chaos suppressing torque. So, taking into account (2.1) and (2.4), the integral (3.46) can be reduced to the form

$$\bar{J}_{\mathcal{NH}} = - \int_{-\infty}^{+\infty} (\bar{\sigma}(t) - \sigma_*) \bar{\sigma}(t) dt = \int_{-\infty}^{+\infty} (\sigma_* - y(t)) y(t) dt$$

Then the condition of the zero-value of the integral $\bar{J}_{\mathcal{NH}}$ can be written as the expression

$$\sigma_* \int_{-\infty}^{+\infty} y(t) dt = \int_{-\infty}^{+\infty} y^2(t) dt$$

and then with the help of (2.6) and (2.7) we obtain the condition of the “insensitivity” of the system’s heteroclinic chaotic dynamics to the influence of the chaos suppressing torque (3.45)

$$2\sigma_*\pi \sqrt{\frac{AB}{(B-\bar{C}_2)(A-\bar{C}_2)}} = \int_{-\infty}^{+\infty} y^2(t) dt \quad (3.52)$$

The analytical expression (3.52) defines sets of the system’s parameters (and also initial conditions) which lead to the undamped heteroclinic chaos; we can use this condition for

analytical finding the “insensitive” parameters – it is the complex task for separated research. We can also numerically evaluate the value of the integral $\bar{J}_{\mathcal{NH}}$. Here, e.g., let us to present the results of the numerical calculations (fig.14) at the parametric variation of the $\bar{\Delta}$ –value and at following inertia-mass parameters (3.48), and for fixed values $p_0 = 1.5$ [1/s], $Q = -15$ [kg·m²/s²].

As can we see, the zero-value of the integral $\bar{J}_{\mathcal{NH}}$ takes place at the value $\tilde{\Delta}^{up} \cong 4$ [kg·m²/s] for the upper separatrix, and at $\tilde{\Delta}^{low} \cong -17$ [kg·m²/s] for the lower separatrix. Therefore, the values $\{\tilde{\Delta}^{up}, \tilde{\Delta}^{low}\}$ define the system’s parameters sets “insensitive” to the chaos suppressing (with the help of the dissipative torque (3.45)), that formally corresponds to the infinitely large value of the “critical” dissipation \bar{e}_σ (3.47), that is, certainly, inappropriate and senselessly for any technical application.

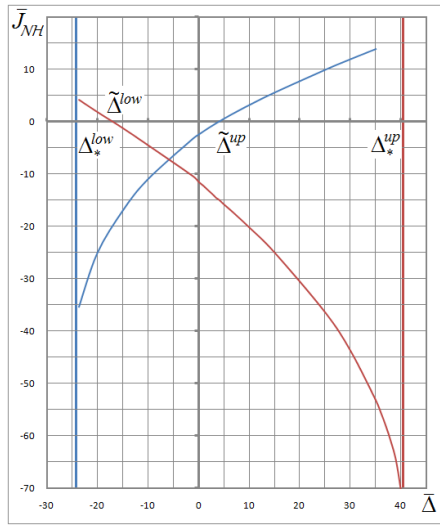


Fig.14. The $\bar{J}_{\mathcal{NH}}$ –value as the dependence on $\bar{\Delta}$: for the upper separatrix – the blue curve; for the lower separatrix – the red curve

Here it is very important to note the “limit” $\bar{\Delta}$ –values $\{\Delta_*^{up}, \Delta_*^{low}\}$ correspond to the bifurcation values which change the type of the heteroclinic polhodes and solutions [Doroshin (2012)]. Also at these values the infinite exponential growth of the magnitude $\bar{J}_{\mathcal{NH}}$ takes place (this is clearly seen from the fig.14). So, these values $\{\Delta_*^{up}, \Delta_*^{low}\}$ in fact are limiting for the typical phase portrait with two heteroclinic separatrices; and exceeding these values lead to the disappearances of the analyzed form of the phase portrait (we will not consider in this work the case after the bifurcation). For this reason all of

the obtained results are applicable in the interval $\bar{\Delta} \in (\Delta_*^{low}, \Delta_*^{up})$.

At the end of the consideration of the described dissipative chaos suppression technique we must underline, that this technique is quite natural, simple and realizable, but it has the big disadvantage for the application to the spin-stabilization of the DSSC in the considering cylindrical precession regime. It is easy to understand, that the energy of the longitudinal rotation of the coaxial DSSC bodies (which is described by the longitudinal angular velocities $r(t)$ and $\sigma(t)$) is decreased at the action of the dissipation (3.45), and for the corresponding conservation of the angular momentum the nutation angle must increase. Moreover, the dissipation can bring the longitudinal angular velocities to the near-zero values, and the nutation angle in this case can achieve quite large amplitude’s values comparable with $\pi/2$. In the practice the last remark means the realization of tilting motions with losses of the spin-stabilized position in the inertial space – this is the worst dynamical result in the framework of the space mission implementation.

Therefore, alternative suppressing techniques are desirable for providing the heteroclinic chaos suppression without the worsening of the DSSC natural dynamics.

The impulse technique of the heteroclinic chaos suppression. Let us introduce into our consideration an impulse technique of the homo/heteroclinic chaos suppression. This technique

is based on generating the small single (or multiple) impulse, which formally is the part of the common interaction of the main body and the rotor of the DSSC, that can be taken into account in the torque (3.20) through the function $F(t)$. In our research we will consider as an example the simplest case of the impulse interaction, when it is formed as the unit-impulse acting between time-moments T_s (the start) and T_f (the finish):

$$\begin{cases} m_{\Delta} = m_{\Delta}(t) = e_F F(t); \\ F(t) = e_F [\text{H}(t - T_s) - \text{H}(t - T_f)] \end{cases} \quad (3.53)$$

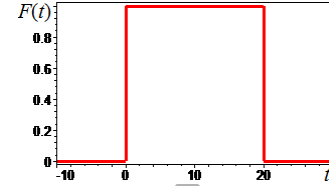


Fig.15. The unit-impulse form

where $\text{H}(t)$ is the Heaviside function. Then we can analytically calculate the corresponding integral (3.28):

$$J_{\mathcal{NH}} = e_F \bar{J}_{\mathcal{NH}}; \quad \bar{J}_{\mathcal{NH}} = \int_{-\infty}^{+\infty} (\bar{\sigma}(t) - \sigma_*) F(t) dt = - \int_{T_s}^{T_f} y(t) dt = \bar{v}_{\delta}(T_s) - \bar{v}_{\delta}(T_f) \quad (3.54)$$

The critical value of the impulse is defined by the value of the coefficient e_F :

$$\bar{e}_F = \sup\{\bar{e}_F^{up}, \bar{e}_F^{low}\}; \quad \bar{e}_F^{sep} = Am(P_{irig}(w_0)) / |\bar{J}_{\mathcal{NH}}^{sep}|; \quad sep = \{up, low\} \quad (3.55)$$

where, as in the previous results, we take into account the both separatrices (upper and lower).

Now it is worth to present the numerical modelling results (Fig.16) for the demonstration of the local regularization (the local chaos suppression) of the dynamics of the DSSC with the following parameters (3.48)-(3.50) at $T_s=0$ [s] and $T_f=20$ [s]. The corresponding critical parameters have the values: $\bar{e}_F^{up} = 1.64539$; $\bar{e}_F^{low} = 0.002$; $\bar{e}_F = 1.64539$.

First of all, from the Poincaré maps (fig.16) we can see the upward relocation of the area of the heteroclinic net (the corresponding chaotic layer) in the phase space with the growth of the e_F -value; also some small relative climb of the right part of the phase portrait takes place. Moreover, the “characteristic size” of the heteroclinic net (the width of the chaotic layer) is decreased with the growth of the parameter e_F . These circumstances mean that the initial heteroclinic net (which is corresponding to the perturbed case without the impulse torque acting) is locally suppressed and extruded up. So, the impulse suppressing technique, in fact, affects the phase space through the small local rising of the positions of the unstable manifolds of the split separatrices and small increasing Δ -values. It also confirms the previous result, that if the rotor speed increases, then the chaotic motion will turn into the regular one [Cheng (2000); Tong (1995)].

It is worth to note here that, in the comparison with the dissipative chaos suppressing technique, the impulse suppressing technique do not change the qualitative form of the phase portrait; and we do not see the “concentrated” Poincaré map (like at the fig.12).

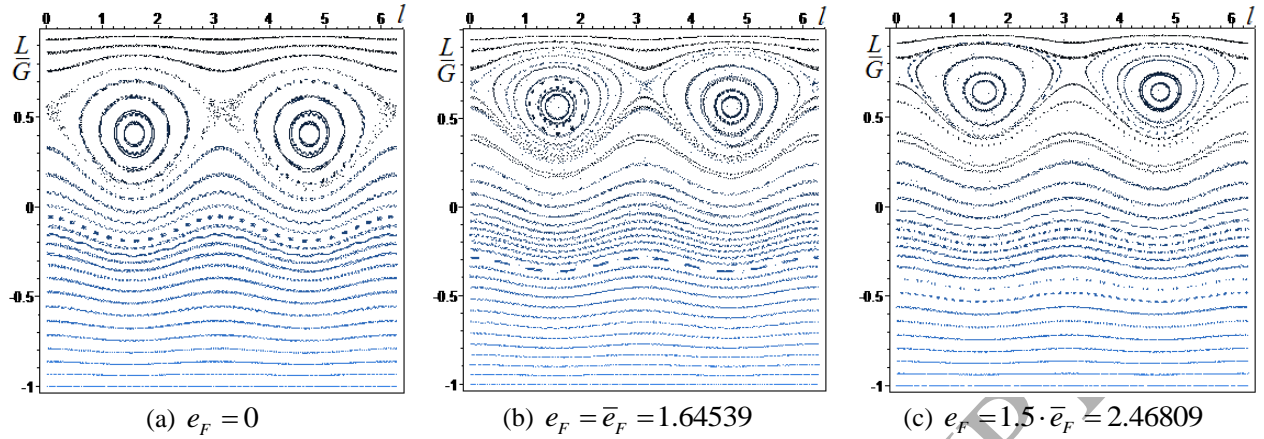


Fig.16. Poincaré sections at the zero (a) /critical (b) / postcritical (c) impulse amplitude

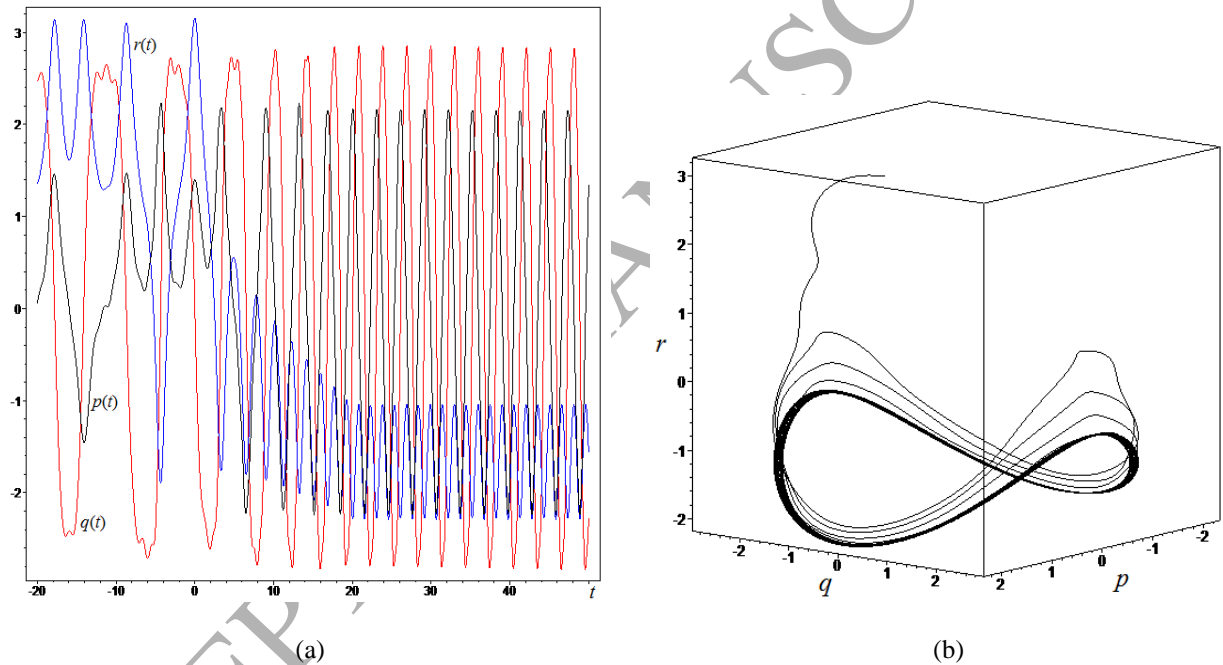


Fig.17. The local angular motion regularization at the critical $e_F = \bar{e}_F = 1.64539$

The presented graphs (last fig.17) shows the regularization of the chaotic motion after the impulse creation – the motion before $t=0$ corresponds to the chaotic regime, which was presented in the previous case (fig.8): we can see the transition to the regular oscillations; also from the figure (fig.16) follows that the heteroclinic net (and the corresponding chaotic layer) is moved to the upper zone of the phase portrait, that rids the initiated regime from the caption into the heteroclinic chaos. Also at the figures (fig.18-a,b and fig.19-a,b) the heteroclinic chaos local suppression in the indicated above Melnikov-Wiggins sense is demonstrated. But at the same time the heteroclinic net in the global scale is preserved, that can be seen from figures' fragments (fig.18-c-f, fig.19-c-f) as the intersections of split manifolds belonging to different heteroclinic trajectories.

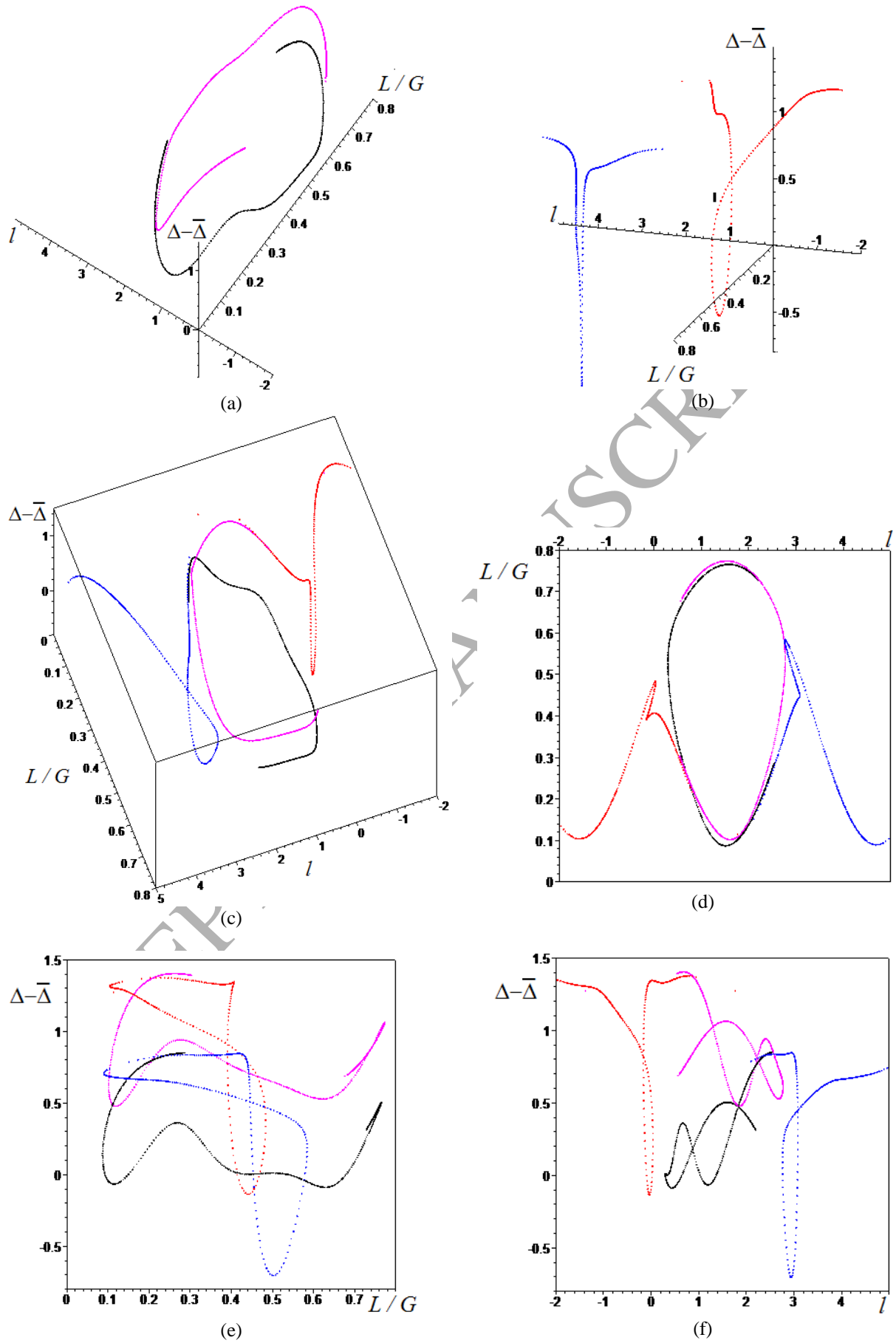


Fig.18. The heteroclinic net fragment as the set of the first Poincaré-images (magenta, red) and the first Poincaré-preimages (black, blue) of the unperturbed separatrices (upper, lower) at the critical \bar{e}_F .

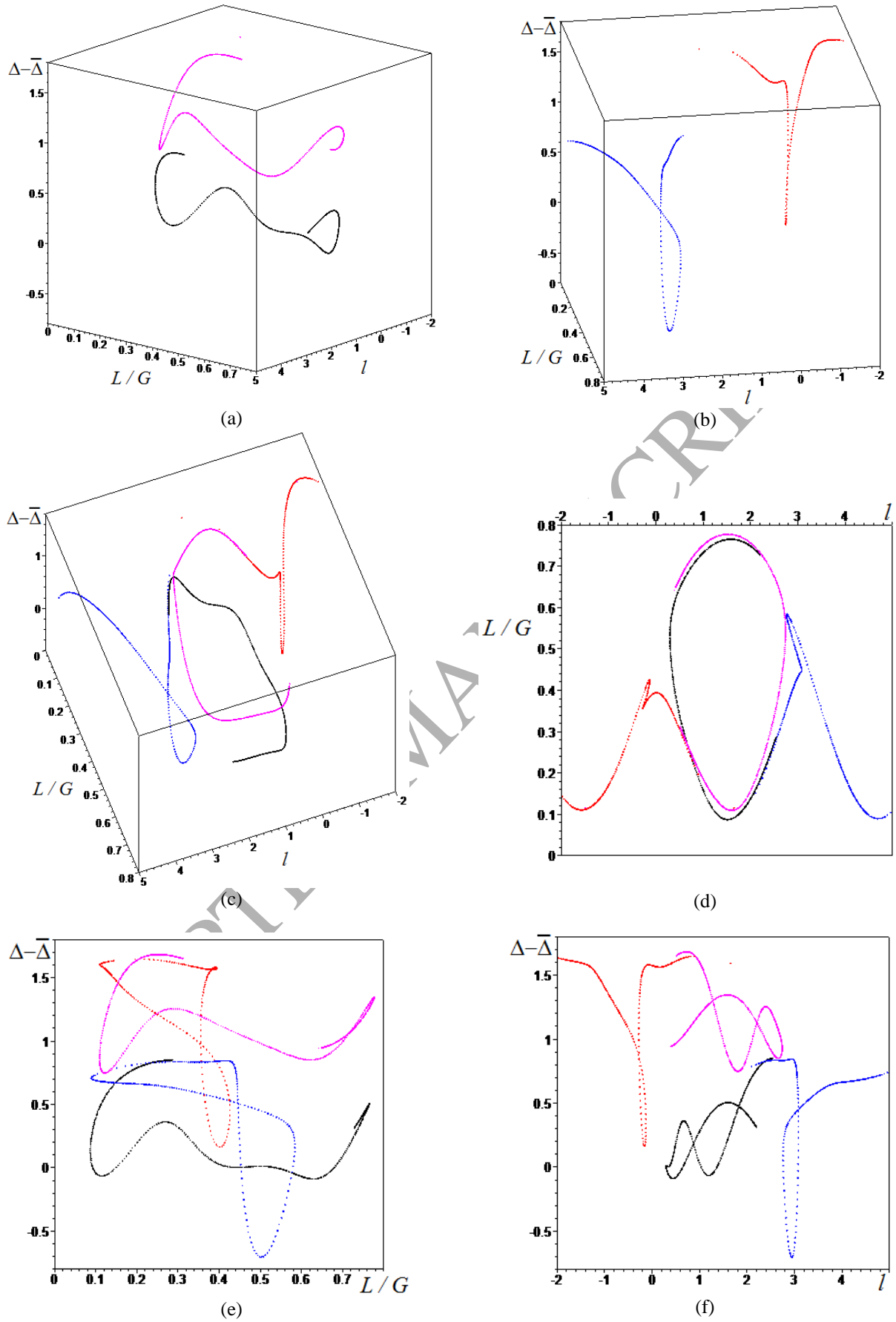


Fig.19. The heteroclinic net fragment as the set of the first Poincaré-images (magenta, red) and the first Poincaré-preimages (black, blue) of the unperturbed separatrices (upper, lower) at the postcritical $e_F = 1.5 \cdot \bar{e}_F$

The limiting case is also interesting, when the boundary time-moments of the impulse switching (on/off) are infinitely separated from each other ($T_s = -\infty$; $T_f = +\infty$). Then the integral follows

$$\bar{J}_{\mathcal{NH}} = - \int_{-\infty}^{+\infty} y(t) dt = -2\pi \sqrt{\frac{AB}{(B-\bar{C}_2)(A-\bar{C}_2)}} \quad (3.56)$$

This case also formally can be applied in the task of the chaos suppression. We can additionally indicate this case as, in fact, the case with the action of the small constant spinup-torque [Neishtadt (2000)]. In [Neishtadt (2000)] the action of such small constant internal spinup-torque was considered in the sense of the negative phenomenon, corresponding to the tilting motion initiation at the separatrix crossing [Neishtadt (2000)]: “The reason is that, during rotor spinup, the phase trajectories of the system, lying on the two-dimensional constant angular momentum surface, may cross an instantaneous separatrix of the unperturbed problem (a gyrostat with a constant relative angular velocity of rotation) and reach qualitatively different domains of final motion” [Neishtadt (2000)]. The indicated reason [Neishtadt (2000)] can be considered as the form of heteroclinic nets arising. This is the negative aspect for the DSSC dynamics, but this aspect is inevitable at the presence of small perturbations, therefore, the realization of the chaotic motion is also inevitable. At the same time, our main aspect of the consideration of small spinup-torque is to develop the chaos suppressing “regularizing” scheme, which can parry the local capture into chaotic regime. In this connection, we can use this spinup impulse torque for local suppressing the heteroclinic net area, and for moving it from the initiated dynamical regime in the phase space. Precisely this ideology follows from the Melnikov-Wiggins formalism as an attempt of the local separation of the split separatrices’ manifolds without their intersections.

It is important to note that the multiple-impulse-technique also can be applied. The corresponding consideration of all aspects of this technique is completely similar to the mono-impulse scheme. Moreover, we can take any complex form of the impulse (linear/polynomial/sinusoidal and other forms).

As the limiting infinitely-multiple-impulse-scheme can be indicated the usual sinusoid or other continuous harmonic/periodical time-functions, but it is clear, that in such cases we obtain (after integrating (3.28)) the harmonic/periodical additional term to the main harmonic Melnikov-Wiggins function’s part $P_{\text{rig}}(w_0)$, instead the constant term like $J_{\mathcal{NH}}$. This result returns us to the pure polyharmonic form of the Melnikov-Wiggins function, and, therefore, the homo/heteroclinic chaos suppression will be impossible – this case we need to consider as the return to the classical dynamical system with chaos at small periodical perturbations.

The magnetic technique of the heteroclinic chaos suppression/avoidance. Let us now consider the motion regularizing approach which differs from the heteroclinic chaos suppressing with the help of the Melnikov-Wiggins methodology. This approach involves the global change of the type of the phase portrait itself, without the construction of functions and conditions of local heteroclinic orbits splitting. So, in order to get out of the chaotic layer area, let us change the internal magnetic properties of the DSSC with simultaneous changing the form of the system phase portrait. The aim here is to move in the changed phase portrait the dangerous heteroclinic region (with the corresponding heteroclinic net) from the current phase trajectory of the initiated dynamical regime. Such relocations of the heteroclinic regions eliminate causes of the heteroclinic chaos initiation.

Together with the initiation of the large angular velocity of the rotor [Cheng (2000); Tong (1995)], an increase of the magnetic torque value (1.47) contributes to the motion regularization. It can be confirmed by the heteroclinic solutions (2.1) and also by the general solutions [Doroshin (2013b)]: from these solutions the presence of the additional “rotational effect” follows, which is described by the corresponding “magnetic term” $E\alpha = \mp\alpha|mB_{orb}|/K$. Moreover, this effect can be considered as the tantamount stabilizing factor [Doroshin (2013b)] in comparison with the gyroscopic stabilization by the large angular velocity of the rotor. So, basing on this dynamical symmetry, we can change in the dynamical sense the gyroscopic stabilization on the magnetic stabilization (and vice versa) – this change is defined by the choice of parameters Δ and E (or we can fully compensate the mutual actions of the magnetic and gyroscopic torques if $\Delta\beta + E\alpha = 0$). Therefore, switching values of the “magnetic term” can provide the natural regularization of the heteroclinic chaos due to the phase portrait’s form replacement with moving the separatrix-region from the initiated dynamical regime.

So, this technique is based on the fast transitions between the natural forms of the system’s phase portraits with using their corresponding dynamical properties. We can present some numerical results for illustration of the indicated technique (fig.20). Here it is needed to define the following form of the magnetic torque ($Q = \pm|mB_{orb}|$):

$$Q = Q_0 + \hat{Q} \left[H(t - T_s) - H(t - T_f) \right] \quad (3.57)$$

that corresponds to switching the DSSC intrinsic magnetic dipole moment (m), where $H(\bullet)$ is the Heaviside function, Q_0 is the initial value of the magnetic torque, T_s, T_f – are the time-moments of the additional magnetic torque \hat{Q} enabling/disabling (the start/finish).

We should give some explanations for our modelling results (fig.20). The components of the angular velocity (frames a₁-d₁) before the initiation of the additional magnetic torque \hat{Q} fulfill the irregular oscillations at $t \in (-\infty, T_s)$ (at the frame c₁ this interval is not depicted). The initiation of the torque \hat{Q} at the time-moment $t = T_s$ changes the current chaotic regime on the regular one. After the torque \hat{Q} disabling at the time-moment $t = T_f$ the current regime can jump to new regular regimes (the frames a, d), or it can proceed to new chaotic modes (the frames b, c). The corresponding polhodes (frames a₂-d₂) were plotted for the time-interval $t \in [T_s, +\infty)$, which include the time-moment $t = T_f$ of the torque \hat{Q} disabling and the subsequent evolutions of the dynamics; these polhodes show us regular modes started at $t = T_s$ with the corresponding jumps to the new regular or chaotic regimes. Also the Poincaré maps (frames a₃-d₃) are very important; these maps are plotted starting at $t = T_s$ and basing on (3.19). The indicated Poincaré maps contain the effects of switching between the forms of the phase portraits.

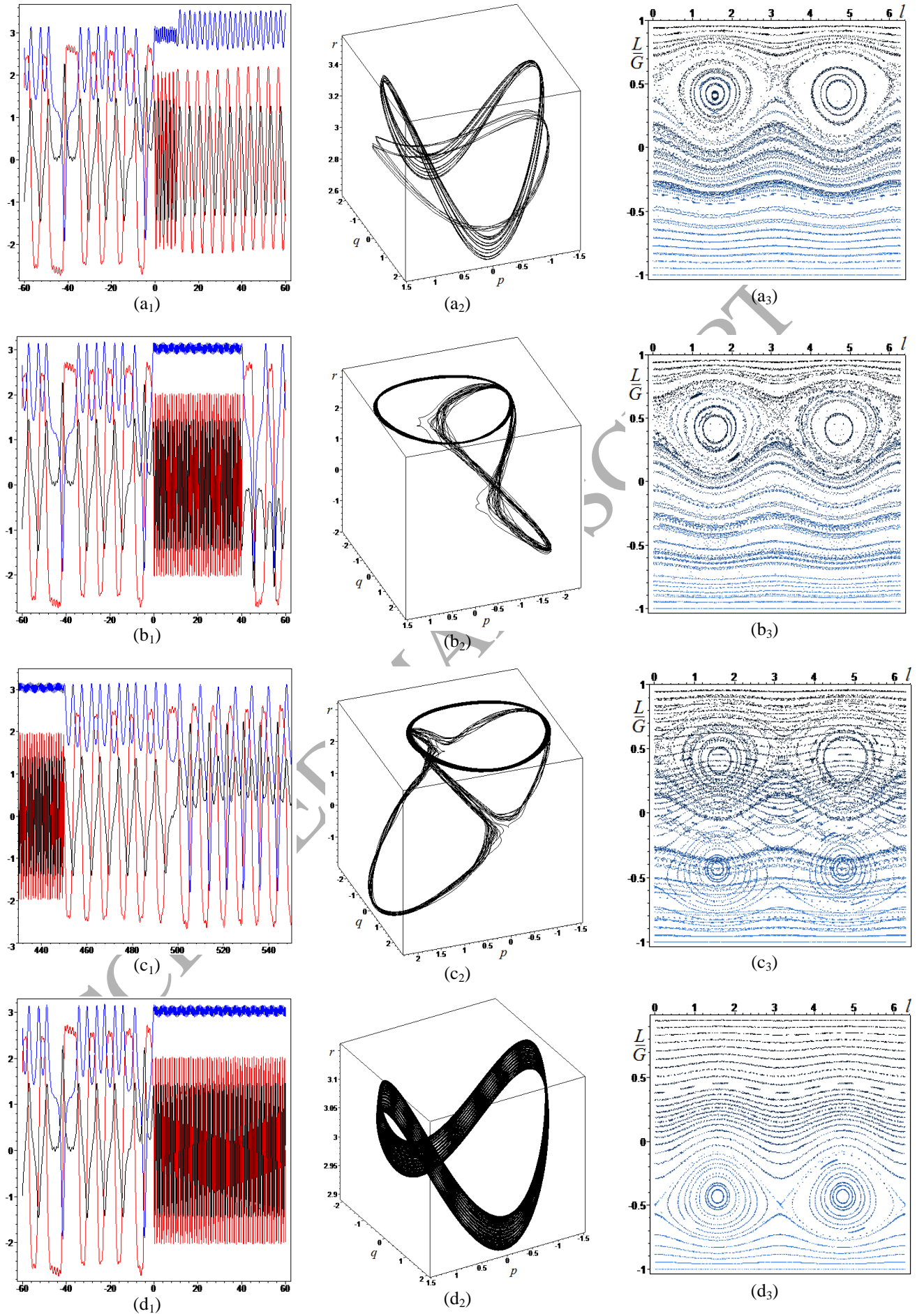


Fig.20. The results of the magnetic technique of the motion regularization

The presented numerical results (Fig.20) were obtained at the parameters from the table.

Table. *The main modelling parameters*

Frames/ regularization types	(a) “the short-time final regularization”	(b) “the short-time regularization with the return to the heteroclinic chaos”	(c) “the long-time regularization with the return to the heteroclinic chaos”	(d) “the permanent final regularization”
\hat{Q} , kg·m ² /s ²	-100	-200	-200	-200
T_s , s	0	0	0	0
T_f , s	10	40	450	$+\infty$
Common parameters	The inertia moments (3.58); $\varepsilon = 0.15$; $e_B = 1$; $e_m = e_\sigma = e_d = e_F = 0$; $p_0 = 1.4$, $q_0 = 0$, $r_0 = 3.15597$, $\sigma_0 = 0.59403$, $\sigma_* = 2.63527$ [rad/s]; $\bar{\Delta} = 15$, $G = 45.29504$ [kg·m ² /s]; $Q_0 = -15$ [kg·m ² /s ²],			

The most interesting case is presented at the frame c_3 (fig.20), where we can see, in fact, the superposition of two classical forms of the system's phase portrait (here the lower blue part of the heteroclinic regions corresponds to the Poincaré-images at $t \in [T_s, T_f]$, and the upper black heteroclinic regions – to the Poincaré-images at $t \in (T_f, +\infty)$). So, these separated in the time parts of the phase portrait represent, per se, the main instrument of the heteroclinic chaos suppression/avoidance – switching between these parts immediately moves away the dangerous heteroclinic region from the current dynamical regime. Certainly, as can we see, the different results can be obtained with the help of the considered “magnetic” technique: the temporary or permanent final chaos suppression/avoidance is possible.

The rotational “spinup-capture” technique of the heteroclinic chaos suppression/avoidance. We can additionally mention one more technique of the possible heteroclinic chaos avoidance at the realization of DSSC motion, based on the rotor-body “spinup-capture” procedure [Doroshin (2009), (2014a,b)] in the three-body-DSSC scheme. For the implementation of this procedure we need add to the considered DSSC-two-body-system the additional opposite “conjugated rotor” (this second rotor can be small and placed into the main DSSC-body). Then in such DSSC-three-body-systems it is possible to fulfill these rotors “conjugate spinup” as the process of the spinup of the conjugated rotors in opposite directions up to desired values of the relative angular velocity with the help of identical internal torques. After this spinup, for instantaneous changing the system phase portrait, we can implement the «opposite rotor capture» (as the immediate stop/deceleration of this rotor relative the main body) – this operation transforms the DSSC-three-body-scheme back to the DSSC-two-body-system, but the main body and the rotor immediately take the modified/redistributed values of the angular momentum at the corresponding “jumping” phase portrait modification. In this way we can immediately move away the dangerous heteroclinic region from the current dynamical regime – this circumstance defines the possibility of the avoidance of the heteroclinic chaos.

Other chaos suppressing techniques and related tasks. Certainly, other chaos controlling/suppressing techniques can be used; most of them have the dissipative nature like the “external/internal resisting medium” [Baozeng Y., Jiafang X.; El-Gohary A.; Iñarra M.;

Kuang J.L.; Leung A.Y.T.; Meechan P.A., Asokanathan S.F.; Zhou L.]. Now, summarizing our descriptions of the DSSC motion investigation, we ought to indicate corresponding well-known problems and results in the framework of the nonlinear regular/chaotic dynamics [Anishchenko V.S., Astakhov V.V. at al.; Bainum P.M. at al.; Beletskii V.V. at al.; Boccaletti S. at al.; Burov A.A.; Celletti A., Lhotka C.; Chaikin S.V.; Doroshin A.V.; Ge Z.-M., Lin T.-N.; Guckenheimer J.; Gutnik S.A.; Hall C.D. at al.; Holmes P. J.; Kinsey K. J.; Lin Yiing-Yuh, Wang Chin-Tzuo; Marsden J.E.; Meechan P.A., Asokanathan S.F.; Meng Y. et al.; Nazari M., Butcher E.A.; Pecora L.M. at al.; Rubanovskii V.M.; Sarychev V.A., Mirer S.A.; Seo at al.; Vera J.A.; Wiggins S.; Zhou at al.], including aspects of the motion stabilizing/detumbling, avoidance of parasitic/spurious harmonics, the system bifurcations, the direct/feedback/time-delayed control (and even the control using neural networks), and, certainly, the chaos synchronization, strange chaotic attractors detecting, etc.

4. Comments and discussions

So, in this work the motion chaotic aspects of the magnetized asymmetric DSSC was considered with the wide use of the Melnikov's-Wiggins' methodology/formalism, which presents the quite effective analytical approach to the homo/heteroclinic chaos detection/suppression. At the same time, some important features of the Melnikov's-Wiggins' methodology must be taken into account.

1). Firstly, for the considered heteroclinic DSSC dynamics we have several separatrices in the phase space (two sets of the "upper" and the "lower" heteroclinic separatrices orbits in the Serret-Andoyer phase-space) – these heteroclinic orbits can be split in different ways, and corresponding heteroclinic chaos can be suppressed at different conditions. Therefore, to analyze of the heteroclinic chaos arising/suppressing we should consider simultaneously and together all of the heteroclinic orbits from the investigated phase space region. Then the final conditions of the chaos suppression follow as "supremal" suppressing values (parameters of the dissipation, impulse magnitudes, etc.) for all heteroclinic orbits.

2). Secondly, the split stable and unstable manifolds of one heteroclinic orbit have not intersections at the fulfilled chaos suppression, but they can have intersections with the split non-intersecting manifolds of other heteroclinic orbits. This circumstance, consequently, preserve the existence of the heteroclinic net in global; and therefore the chaos in global is not suppressed (as opposed to homoclinic cases). Certainly, this heteroclinic net will differ from the corresponding one before the action of suppressing factors; but in any case, we can take as the result the changed location and changed properties of the chaotic layer in the phase space, so the chaotic dynamics does not vanish in global. The further evolution of the changed heteroclinic net at the action of suppressing factors in global, generally speaking, is indeterminate.

3). In the third place, it is well-known fact, that at the construction of the Melnikov's formalism [Melnikov; Arnold; Wiggins] the dynamical conditions for the homo/heteroclinic trajectories on infinite limits ($t = \pm\infty$) are very important. In the homoclinic cases these conditions are equal: homoclinic trajectories start and finish in the single original homoclinic point, so the "distances" between the unperturbed original homoclinic point and perturbed one is the same at $t = +\infty$ and at $t = -\infty$. But for heteroclinic cases these dynamical conditions on

infinite limits can be differ so far as the heteroclinic trajectories start (at $t = -\infty$) in one point and finish (at $t = +\infty$) in the another point; and, moreover, distances between their unperturbed and corresponding perturbed positions are not obliged to be equal. So, for the heteroclinic cases the guaranteed fulfillment of the Melnikov's formalism is possible at the additional conditions of the equality of distances between unperturbed and perturbed positions of the two different heteroclinic points (e.g. at the "symmetry" of deformations of the split manifolds of heteroclinic trajectory, and of the whole phase portrait). In the general case for heteroclinic trajectories this additional conditions are not fulfilled *a priori*.

Taking into account mentioned above features and difficulties of the Melnikov's-Wiggins' formalism we must note that the application of this methodology to the analysis of the DSSC chaotic dynamics is necessary in any case, at least, in the framework of the primordial research. It is also worth to construct the alternative additional analytical techniques of the heteroclinic chaos study.

5. Conclusion

In the paper the chaotic dynamics of the perturbed attitude motion of the magnetized DSSC with the complex general form of the constructional/mass-inertia asymmetry at the implementation of important regimes (including the cylindrical precessions on equatorial circle orbits of the Earth) was investigated basing on the Melnikov-Wiggins methodology. The corresponding simple polyharmonic structure of the Melnikov-Wiggins function was written for cases of Hamiltonian and non-Hamiltonian perturbations. Some heteroclinic chaos suppressing dissipative techniques were analyzed, including actions of natural forces/torques (the friction between the coaxial DSSC bodies, internal electromotor's torques, counterelectromotive force/torques in the DSSC internal electromotor) and also some alternative suppressing techniques were suggested, including the creation of internal magnetic impulses, and the implementation of the DSSC conjugate rotors "spinup-capture" dynamics. All of them can be used as the natural instruments for the DSSC motion parameters changing and for the chaos control/avoidance.

Acknowledgments

This work is partially supported by the Russian Foundation for Basic Research (RFBR#15-08-05934-A), and by the Ministry education and science of the Russian Federation (in the framework of the design part of the State Assignments to higher education institutions and research organizations in the field of scientific activity – project #9.1004.2014/K).

References

- Andoyer H. (1923), *Cours de Mecanique Celeste*, Paris: Gauthier-Villars.
- Anishchenko V.S., Astakhov V.V., Neiman A.B., Vadivasova T.E., Schimansky-Geier L. (2007), *Nonlinear Dynamics of Chaotic and Stochastic Systems. Tutorial and Modern Development*. Springer-Verlag, Berlin.
- Arkhangelskiĭ U.A. (1977), *Analytical rigid body dynamics*. Nauka, Moscow.
- Arnold V.I. (1964), Instability of dynamical systems with several degrees of freedom, *Doklady Akademii Nauk SSSR*, 156 (1), pp. 9-12.
- Aslanov V.S. (2012), Integrable cases in the dynamics of axial gyrostats and adiabatic invariants, *Nonlinear Dynamics*, Volume 68, Numbers 1-2, pp. 259-273.
- Aslanov V.S., Doroshin A.V. (2002), Stabilization of a reentry vehicle by a partial spin-up during uncontrolled descent. *Cosmic Research* 40 (2), pp. 178-185.
- Aslanov V.S., Doroshin A.V. (2010), Chaotic dynamics of an unbalanced gyrostat. *Journal of Applied Mathematics and Mechanics*, Volume 74, Issue 5, pp.525-535.
- Aslanov V.S., Yudintsev V.V. (2012), Dynamics and chaos control of gyrostat satellite, *Chaos, Solitons & Fractals* 45, pp.1100–1107.
- Aslanov V.S., Yudintsev V.V. (2013), Dynamics and control of dual-spin gyrostat spacecraft with changing structure, *Celestial Mechanics and Dynamical Astronomy*, Volume 115, Issue 1, pp. 91-105.
- Aslanov V.S., Yudintsev V.V. (2014), Dynamics and Chaos Control of Asymmetric Gyrostat Satellites, *Cosmic Research*, Vol. 52, No. 3, pp. 216–228.
- Bainum P. M., Fuechsel P. G., Mackison D. L. (1970), Motion and Stability of a Dual-Spin Satellite With Nutation Damping, *Journal of Spacecraft and Rockets*, Vol. 7, No. 6, pp. 690-696.
- Bao-Zeng Y., Jiafang X. (2007), Chaotic attitude maneuvers in spacecraft with a completely liquid-filled cavity, *Journal of Sound and Vibration* 302, pp. 643–656.
- Baozeng Y., Jiafang X. (2007), Chaotic attitude maneuvers in spacecraft with a completely liquid-filled cavity, *Journal of Sound and Vibration* 302, pp. 643–656.
- Bao-Zeng Yue (2008), Heteroclinic bifurcations in completely liquid-filled spacecraft with flexible appendage, *Nonlinear Dyn* 51:317–327.
- Bao-Zeng Yue (2011), Study on the Chaotic Dynamics in Attitude Maneuver of Liquid-Filled Flexible Spacecraft, *AIAA Journal*, Vol. 49, No. 10, pp. 2090-2099.
- Beletskii V.V., Pivovarov M.L., Starostin E.L. (1996), Regular and chaotic motions in applied dynamics of a rigid body. *Chaos* 6 (2).
- Beletsky V.V. (1995), *Reguläre und chaotische Bewegung starrer Körper*. Teubner.
- Boccaletti S., Kurths J., Osipov G., Valladares D.L., Zhou C.S. (2002), The synchronization of chaotic systems. *Physics Reports* 366, pp. 1–101.
- Burov A.A. (2013), Conservative methods of controlling the rotation of a gyrostat, *Journal of Applied Mathematics and Mechanics* 77, pp.195– 204.
- Celletti A., Lhotka C. (2014), Transient times, resonances and drifts of attractors in dissipative rotational dynamics, *Commun. Nonlinear Sci. Numer. Simulat.* 19, pp. 3399–3411.
- Chaikin S.V. (2013), Bifurcations of the relative equilibria of a gyrostat satellite for a special case of the alignment of its gyrostatic moment, *Journal of Applied Mathematics and Mechanics* 77, pp. 477– 485.
- Chen H.-K. (2002), Chaos and chaos synchronization of a symmetric gyro with linear-plus-cubic damping, *Journal of Sound and Vibration* (2002) 255(4), pp. 719-740.
- Chen Li-Qun, Liu Yan-Zhu (2002), Chaotic attitude motion of a magnetic rigid spacecraft and its control, *International Journal of Non-Linear Mechanics* 37, pp. 493–504.
- Chen Li-Qun, Liu Yan-Zhu, Cheng Gong (2002), Chaotic attitude motion of a magnetic rigid spacecraft in a circular orbit near the equatorial plane, *Journal of the Franklin Institute* 339, pp. 121–128.
- Cheng G. and Liu Y. Z. (2000), Chaotic motion of an asymmetric gyrostat in the magnetic field of the earth, *Acta Mechanica* 141, pp.125-134.

- Chinnery A. E., Hall C. D. (1995), Motion of a Rigid Body with an Attached Spring-Mass Damper, *J. Guidance Control Dyn.* Vol. 18, No. 6, pp.1404-1409.
- Cochran, J.E., Shu, P.H., Rew, S.D. (1982), Attitude motion of asymmetric dual-spin spacecraft. *J. Guid. Control Dyn.* 5, pp.37-42.
- Deprit A. (1967), A free rotation of a rigid body studied in the phase plane, *American Journal of Physics* 35, pp.424-428.
- Doroshin A.V. (2008a), Evolution of the Precessional Motion of Unbalanced Gyrostats of Variable Structure. *Journal of Applied Mathematics and Mechanics* 72, pp. 259-269.
- Doroshin A.V. (2008b), Synthesis of Attitude Motion of Variable Mass Coaxial Bodies, *WSEAS Transactions on systems and control*, Issue 1, Volume 3, pp. 50-61.
- Doroshin A.V. (2009), Attitude Control of Spider-type Multiple-rotor Rigid Bodies Systems. *Proceedings of the World Congress on Engineering 2009*, London, U.K. Vol II, pp.1544-1549.
- Doroshin A.V. (2010), Analysis of attitude motion evolutions of variable mass gyrostats and coaxial rigid bodies system, *International Journal of Non-Linear Mechanics*, Volume 45, Issue 2, pp. 193-205.
- Doroshin A.V. (2011), Modeling of chaotic motion of gyrostats in resistant environment on the base of dynamical systems with strange attractors, *Communications in Nonlinear Science and Numerical Simulation*, Volume 16, Issue 8, pp. 3188-3202.
- Doroshin A.V. (2012), Heteroclinic dynamics and attitude motion chaotization of coaxial bodies and dual-spin spacecraft, *Communications in Nonlinear Science and Numerical Simulation*, Volume 17, Issue 3, pp. 1460-1474.
- Doroshin A.V. (2013a), Exact solutions for angular motion of coaxial bodies and attitude dynamics of gyrostatt-satellites. *International Journal of Non-Linear Mechanics*, Volume 50, pp. 68-74.
- Doroshin A.V. (2013b), Exact Solutions in Attitude Dynamics of a Magnetic Dual-Spin Spacecraft and a Generalization of the Lagrange Top, *WSEAS Transactions on systems*, Issue 10, Volume 12, pp. 471-482.
- Doroshin A.V. (2014a), Chaos and its avoidance in spinup dynamics of an axial dual-spin spacecraft, *Acta Astronautica*, Volume 94, Issue 2, pp. 563-576.
- Doroshin A.V. (2014b), Homoclinic solutions and motion chaotization in attitude dynamics of a multi-spin spacecraft, *Communications in Nonlinear Science and Numerical Simulation*, Volume 19, Issue 7, pp. 2528-2552.
- Doroshin A.V. (2014c), Multi-spin spacecraft and gyrostats as dynamical systems with multiscroll chaotic attractors, *Proceedings of 2014 Science and Information Conference*, SAI 2014, pp. 882-887.
- Doroshin A.V., Krikunov M.M. (2014), Attitude Dynamics of a Spacecraft with Variable Structure at Presence of Harmonic Perturbations, *Appl. Math. Modelling*, Volume 38, Issues 7-8, pp. 2073-2089.
- Doroshin A.V. (2015), Heteroclinic chaos in attitude dynamics of a dual-spin spacecraft at small oscillations of its magnetic moment, *WSEAS Transactions on systems*. In press.
- El-Gohary Awad (2005), Optimal control of damping rotation of a rigid body using fly wheels with friction, *Chaos, Solitons and Fractals* 24, pp. 207-221.
- El-Gohary Awad (2006), New control laws for stabilization of a rigid body motion using rotors system, *Mechanics Research Communications*, Volume 33, Issue 6, pp. 818-829.
- El-Gohary Awad (2009), Chaos and optimal control of steady-state rotation of a satellite-gyrostatt on a circular orbit, *Chaos, Solitons & Fractals*, Volume 42, pp. 2842-2851.
- Elipse A., Lanchares V. (2008), Exact solution of a triaxial gyrostatt with one rotor, *Celestial Mechanics and Dynamical Astronomy*, Issue 1-2, Volume 101, pp. 49-68.
- Ge Z.-M., Lin T.-N. (2002), Chaos, Chaos Control And Synchronization Of A Gyrostatt System, *Journal of Sound and Vibration*, Volume 251, Issue 3, pp. 519-542.
- Ge Z.-M., Lin T.-N. (2003), Chaos, Chaos Control And Synchronization Of Electro-Mechanical Gyrostatt System, *Journal of Sound and Vibration* 259(3), pp. 585-603.
- Golubev V.V. (1953), *Lectures on Integration of the Equations of Motion of a Rigid Body about a Fixed Point*. Moscow: State Publishing House of Theoretical Literature.
- Guckenheimer J., Holmes P. (1983), *Nonlinear Oscillations, Dynamical Systems, and Bifurcation of Vector Fields*, Springer, Berlin.

- Guirao J.L.G., Vera J.A. (2010), Dynamics of a gyrostat on cylindrical and inclined Eulerian equilibria in the three-body problem, *Acta Astronautica* 66, pp. 595 - 604.
- Gutnik S.A., Sarychev V.A. (2014), Dynamics of an axisymmetric gyrostat satellite. Equilibrium positions and their stability, *Journal of Applied Mathematics and Mechanics* 78, pp. 249–257.
- Hall C. D. (1997), Momentum Transfer Dynamics of a Gyrostat with a Discrete Damper, *J. Guidance Control Dyn.*, Vol. 20, No. 6, pp. 1072-1075.
- Hall C. D. (1998), Escape from gyrostat trap states, *J. Guidance Control Dyn.* 21, pp. 421-426.
- Hall C.D., Rand R.H. (1994), Spinup Dynamics of Axial Dual-Spin Spacecraft, *Journal of Guidance, Control, and Dynamics*, Vol. 17, No. 1, pp. 30–37.
- Holmes P. J., Marsden J. E. (1983), Horseshoes and Arnold diffusion for Hamiltonian systems on Lie groups, *Indiana Univ. Math. J.* 32, pp. 273-309.
- Holms P. J. (1990), Poincaré, celestial mechanics, dynamical-systems theory and chaos – *Physics Reports (Review Section of Physics Letters)* 193, No. 3, pp. 137—163 (North-Holland).
- Iñarraea M. (2009), Chaos and its control in the pitch motion of an asymmetric magnetic spacecraft in polar elliptic orbit// *Chaos, Soliton and Fractals* 40, pp. 1637-1652.
- Iñarraea M., Lanchares V. (2000), Chaos in the reorientation process of a dual-spin spacecraft with time-dependent moments of inertia, *International Journal of Bifurcation and Chaos*, Vol. 10, No. 5, pp. 997-1018.
- Iñarraea M., Lanchares V., Rothos V. M., Salas J. P. (2003), Chaotic rotations of an asymmetric body with time-dependent moment of inertia and viscous drag, *International Journal of Bifurcation and Chaos*, Vol. 13, No. 2, pp. 393-409.
- Ivin E.A. (1985), Decomposition of variables in task about gyrostat motion, *Mathematics and Mechanics series*, no.3, *Vestnik MGU (Transactions of Moscow's University)*, pp.69–72.
- Kinsey K. J., Mingori D. L., Rand R. H. (1996), Non-linear control of dual-spin spacecraft during despin through precession phase lock, *J. Guidance Control Dyn.* 19, pp. 60-67.
- Kozlov V.V. (1980), *Methods of Qualitative Analysis in the Dynamics of a Rigid Body*, Gos. Univ., Moscow.
- Kuang J.L., Meehan P.A., Leung A.Y.T. (2006a), On the chaotic rotation of a liquid-filled gyrostat via the Melnikov–Holmes–Marsden integral, *International Journal of Non-Linear Mechanics* 41, pp. 475 – 490.
- Kuang J.L., Meehan P.A., Leung A.Y.T. (2006b), Suppressing chaos via Lyapunov–Krasovskii's method, *Chaos, Solitons and Fractals* 27, pp. 1408–1414.
- Kuang Jinlu, Tan Soonhie, Arichandran Kandiah, Leung A.Y.T. (2001), Chaotic dynamics of an asymmetrical gyrostat, *International Journal of Non-Linear Mechanics* 36, pp. 1213-1233.
- Leung A. Y. T., Kuang J. L. (2004), Spatial chaos of 3-D elastica with the Kirchhoff gyrostat analogy using Melnikov integrals, *Int. J. Numer. Meth. Eng.* 61, pp.1674–1709.
- Leung A.Y.T., Kuang J.L. (2007), Chaotic rotations of a liquid-filled solid, *Journal of Sound and Vibration* 302, pp. 540–563.
- Likins P. W. (1986), *Spacecraft Attitude Dynamics and Control - A Personal Perspective on Early Developments*, *J. Guidance Control Dyn.* Vol. 9, No. 2, pp. 129-134.
- Lin Yiing-Yuh, Wang Chin-Tzuo (2014), Detumbling of a rigid spacecraft via torque wheel assisted gyroscopic motion, *Acta Astronautica* 93, pp. 1–12.
- Meehan P.A., Asokanthan S.F. (2002), Control of chaotic instabilities in a spinning spacecraft with dissipation using Lyapunov's method, *Chaos, Solitons and Fractals* 13, pp. 1857-1869.
- Melnikov V.K. (1963), On the stability of the centre for time-periodic perturbations, *Trans. Moscow Math. Soc.* No.12, pp. 1-57.
- Meng Y., Hao R., Chen Q. (2014), Attitude stability analysis of a dual-spin spacecraft in halo orbits, *Acta Astronautica* 99, pp. 318–329.
- Mingori D. L. (1969), Effects of Energy Dissipation on the Attitude Stability of Dual-Spin Satellites, *AIAA Journal*, Vol. 7, No. 1, pp. 20-27.
- Nazari M., Butcher E.A. (2014), On the stability and bifurcation analysis of dual-spin spacecraft, *Acta Astronautica* 93, pp.162–175.

- Neishtadt A.I., Pivovarov M.L. (2000), Separatrix crossing in the dynamics of a dual-spin satellite. *Journal of Applied Mathematics and Mechanics*, Volume 64, Issue 5, pp. 709-714.
- Or A.C. (1998a), Chaotic Motions of a Dual-Spin Body, *Transactions of the ASME*, Vol.65, pp. 150-156.
- Or A.C. (1998b), Dynamics of an Asymmetric Gyrostat, *Journal of Guidance, Control, and Dynamics*, Vol.21, No.3, pp. 416-420.
- Pecora L.M., Carroll T.L., Johnson G.A., Mar D.J. (1997), Fundamentals of synchronization in chaotic systems, concepts, and applications. *Chaos* 7 (4), pp. 520-543.
- Peng J., Liu Y. (2000), Chaotic motion of a gyrostat with asymmetric rotor, *International Journal of Non-Linear Mechanics*, Volume 35, Issue 3, pp. 431-437.
- Poincaré, H. (1899), *Les Methodes Nouvelles de La Mécanique Celeste*, Vols. 1-3 (Gauthier Villars, Paris).
- Rubanovskii V.M. (1991), Bifurcation and stability of the relative equilibria of a gyrostat satellite, *Journal of Applied Mathematics and Mechanics*, Volume 55, Issue 4, pp. 450-455.
- Sadov Y.A. (1970), The action-angle variables in the Euler-Poinsot problem, *Journal of Applied Mathematics and Mechanics*, vol. 34, issue 5, pp. 922-925 (*PMM "Prikladnaja matematika i mehanika"*, vol.34, №5, pp. 962-964).
- Sandfry R.A., Hall C.D. (2007), Bifurcations of relative equilibria of an oblate gyrostat with a discrete damper, *Nonlinear Dyn* 48, pp. 319-329.
- Sarychev V.A., Mirer S.A., Isakov A.V. (1981), Dual-spin satellites with gyro-damping, *Acta Astronautica*, Volume 9, Issue 5, pp. 285-289.
- Sarychev V.A., Mirer S. A. (2001), Relative equilibria of a gyrostat satellite with internal angular momentum along a principal axis, *Acta Astronautica* Vol. 49, No. 11, pp. 641- 644.
- Seo In-Ho, Leeghim Henzeh, Bang Hyochoong (2008), Nonlinear momentum transfer control of a gyrostat with a discrete damper using neural networks, *Acta Astronautica* 62, pp. 357 - 373.
- Serret, J. A. (1866), Mémoire sur l'emploi de la méthode de la variation des arbitraires dans la théorie des mouvements de rotation. *Mémoires de l'Académie des Sciences de Paris*, Vol. 55, pp. 585-616.
- Shirazi K.H., Ghaffari-Saadat M.H. (2004), Chaotic motion in a class of asymmetrical Kelvin type gyrostat satellite, *International Journal of Non-Linear Mechanics*, Volume 39, Issue 5, pp. 785-793.
- Tabor M., *Chaos and Integrability in Nonlinear Dynamics: An Introduction*. Wiley, John & Sons, New York, 1989.
- Tong X., Tabarrok B. (1995), Chaotic motion of an asymmetric gyrostat in the gravitational field, *International Journal of Non-Linear Mechanics* Volume 30, Issue 3, pp.191-203.
- Vera J.A. (2013), The gyrostat with a fixed point in a Newtonian force field: Relative equilibria and stability, *J. Math. Anal. Appl.* 401, pp. 836-849.
- Wiggins S. (1988), *Global Bifurcations and Chaos : Analytical Methods (Applied mathematical sciences : vol. 73)*. Springer-Verlag.
- Wiggins S., Shaw S.W. (1988), Chaos and Three-Dimensional Horseshoes in Slowly Varying Oscillators, *Journal of Applied Mechanics*, Vol.55, pp. 959-968.
- Wiggins S. (1990), *Introduction to applied nonlinear dynamical systems and chaos*. Springer-Verlag.
- Wiggins S. (1992), *Chaotic Transport in Dynamical Systems*. Springer-Verlag.
- Wittenburg J. (1975), *Beitrage zur dynamik von gyrostaten*, *Accademia Nazionale dei Lincei, Quaderno N. 227*.
- Wittenburg J. (1977), *Dynamics of Systems of Rigid Bodies*. Stuttgart: Teubner.
- Zhou L., Chen Y., Chen F. (2009), Stability and chaos of a damped satellite partially filled with liquid, *Acta Astronautica* 65, pp. 1628-1638.